Dynamic Mutual Capacitive Sensor for Human Interactions.

A Dissertation Presented for the

Doctor of Philosophy

Degree

The University of Tennessee, Knoxville

Jonathan William Huber

May 2013

Dedication

Dedicated to my supporters

To my wife Laura, thank you for doing everything I couldn't.

I love you.

Acknowledgements

To get this far I needed the support of my family, friends, and colleagues. One doesn't get this far alone. Without my parents pushing me through my pre-college days or my wife's understanding of return to school, I never would have reached this point. That being said, there are a select number of individuals that help me transition from student to candidate.

It started with Ron Nutt who granted me the Ronald Nutt Fellowship for Distinguished Fellows. It wasn't easy to award a non-electrical engineer. There was a lot of paperwork. I appreciate the award because it helped validate my professional experiences that I had gained. I felt as though it made me a bit more than a run of the mill Non-Traditional Student.

Next I met Dr. Mohamed Mahfouz. I took his class on image processing for medical applications. Once again, someone took a chance on me. He offered me an opportunity to study capacitive pressure sensors, but it turned into learning about a wide range of next generation biomedical technologies. One of the more valuable pieces of gained knowledge came from seeing an entrepreneur develop technologies in a university environment. This is one of my ultimate goals and it was good to witness his methodology. I can say many of the same things about Dr. Richard Komistek. But I will add that he was always there to back me up when I needed it.

While mentoring senior design groups, I was able to listen to Dr. William Hamel coach the different team members. I especially learned from watching him talk with some of my more difficult students. It was always a good blend of being stern and communicating the point while remaining constructive. It was good to witness the message.

Coming into to school I knew I needed to learn how to write research grants. I didn't realize how real of an opportunity I would get when I signed up Dr. H. Lee Martin's technology in entrepreneurship class. He taught me the difference between dreaming big and dreaming epic. And then he enabled me to try. I wrote a SBIR, business plans, and numerous lines of

code in pursuit of being an entrepreneur. It's great to talk with someone who looks you in the eye and says "I dare you".

I must also pay homage to Dr. Roger Parsons, Dr. Chris Pionke, and Dr. John Landis. I've known you for a long time and you've always made time for me. Don't worry, just because I'm graduating doesn't mean I won't randomly stop by and see you.

Finally, just a small thanks to a few professors I've met along the way: Dr. Baker, Dr. Bennett, Dr. Boulet, Dr. Irick, Dr. Matthews, both Dr. Scotts, Dr. Solomon, and Dr. Zhao.

Thank you all.

Abstract

This dissertation introduces the novel concept of removing the ground conductive plate by utilizing body capacitance as the ground in the capacitive sensor, whereby circuit pressure sensing can occur with only one plate and one dielectric. Additionally, body capacitance sensing was limited to a binary touch-no-touch output, whereas the method presented here can sense various applied pressures. The resulting circuit acts as an antenna that receives local capacitance signals from a human interaction.

The advantage of this design is that it allows for both proximity sensing and pressure sensing (once the body part is touching the dielectric material). This setup is ideal for a z-axis dimensional interface for touchscreen devices, as well as pressure sensing palpation or planter region interaction.

Preface

This dissertation is the introduction to using mutual capacitance from a human performing proximity and pressure sensing using a conductive plate(s) of any size. The fundamental mechanics of this interaction are explored including a Capacitance-to-Digital Conversion (CDC) microcontroller evaluation with data acquisition, Material stress-strain Instron testing with differential capacitance measurements for various elastic dielectrics, palpation relative and absolute proximity and pressure sensing, and plantar proximity and pressure sensing for gait detection.

Table of Contents

Chapter 1 Contributions *1*

Section 1.1 Fundamental Contributions **4**

Part 1.1.1 Capacitive Proximity and Pressure Sensing of Human Interaction 4

Part 1.1.2 Laser Cut Flexible Sensor 8

Chapter 2 Background *11*

Section 2.1 Capacitive Proximity and Pressure Sensing Mathematical Relationships **11**

Section 2.2 The Pedobarographic Gait Shoe **13**

Part 2.2.1 Center of Pressure Monitoring 13

Part 2.2.2 Electronic On-Shoe Pedobarography 14

Part 2.2.3 Design Objectives for Capacitive Shoe Insole Sensor 16

Chapter 3 Design and Methods *17*

Section 3.1 Controller Hardware **22**

Part 3.1.1 Single Microcontroller with CDC 23

Part 3.1.2 Multi-MicroController MISO Connectivity 24

Part 3.1.3 Multiplexor PCB with MicroController 25

Section 3.2 Selection of Sensor Dielectric Material **26**

Section 3.3 Sensor Fabrication Methods **31**

Part 3.3.1 Simple Copper Plates and PCB Etchant 31

Part 3.3.2 Lithography Flexible Sensor 33

Part 3.3.3 Laser-Cut Aluminum Foil Sensor Array 35

Section 3.4 Data Analysis **38**

Part 3.4.1 Data Acquisition Graphical User Interface (GUI) and Real-time Display 38

Part 3.4.2 Method 38
Part 3.4.3 Data Acquisition Results 41
Part 3.4.4 Summary of Data Acquisition and GUI Frame Rates 43

***Chapter 4 Results* 44**

Section 4.1 Palpation Proximity and Pressure Sensing Results 44

Section 4.2 Plantar Proximity and Pressure Sensing Gait Detection Results 48

***Chapter 5 Discussion* 54**

***Chapter 6 Future Work* 58**

***List of References* 60**

***Vita* 63**

List of Tables

Table 1. Proximity Sensing Benchmarks 3

Table 2. Summary of gait detection methods and sensor location 15

Table 3. List of dielectric properties 28

Table 4. Comparison of sensor array fabrication methods 37

List of Figures

Figure 1. Leon Theremin using mutual capacitance to control volume and pitch. 2

Figure 2. Diagram of the proposed proximity and pressure sensor utilizing body capacitance with a microcontroller to interpret the capacitance values. 6

Figure 3. The single capacitive plate used as a proximity and pressure sensor. 6

Figure 4. Sensor position inside the shoe through a typical gait. 7

Figure 5. Capacitive sensor response from a typical gait. Image from http://www.med.nyu.edu/rehabengineering/research/locomotion.html..... 7

Figure 6. The laser cut sensor process from CAD drawing: to cut, to connection to the microcontroller. 9

Figure 7. Diagram and equations exhibiting stacked dielectrics act in series. 12

Figure 8. Process to convert a relative proximity and pressure sensor into an absolute sensor. 19

Figure 9. The fundamental concept of mutual capacitance proximity and pressure sensing. . 20

Figure 10. Test set-up to establish fixed proximity points and subsequent transition to pressure sensing. 21

Figure 11. Silicon Labs C8051F996 microcontroller [25] 23

Figure 12. Basic MISO schematic 24

Figure 13. MISO Master PCB: concept and fabrication 25

Figure 14. Sensor array PCB for multiplexor 26

Figure 15. General Capacitive equations as a ratio of electric potential strain to mechanical strain. Data collected for Polyurethane shown. 29

Figure 16. Cyclic loading of capacitive sensor during Instron compression testing. 30

Figure 17. Test setup to evaluate C8051F996 mircocontroller's ability to perform CDC array sensing with a multiplexor. 32

Figure 18. Sensor row number, column number, and sensor's overlapping area. The microcontroller is compatible with multiplexor array sensing. 32
Figure 19. Design strategy for flexible sensor array 34
Figure 20. Flexible sensor array design and fabrication..... 34
Figure 21. The laser-cut sensor process: CAD drawing, cutting, and connecting to microcontroller 36
Figure 22. Sensor data collection GUI..... 40
Figure 23. Sensor data collection program flow..... 40
Figure 24. Data collection frame rates..... 42
Figure 25. Data collection frame rates per specific function..... 43
Figure 26. Mutual capacitance increase of a finger approaching a dielectric and capacitive plate. 46
Figure 27. Pressure sensing tests for CDC counts-to-load relationship. 47
Figure 28. Mutual capacitance proximity and pressure sensing, relative to absolute transition. 48
Figure 29. Layout of plantar sensors..... 50
Figure 30. Plantar region mutual capacitive gait unfiltered data. Standing, walking 10 steps, and then standing. 50
Figure 31. Data filtered with a 20 point moving average. This value is acceptable for general gait detection, but may vary by the particular aspect of the gait being studied. 51
Figure 32. Gait events can be detected with a plantar mutual capacitance sensor: 1) Heel Strike, 2) Metatarsal Contact, 3) Big Toe Contact, 4) Big Toe Lift-off, 5) Swing, and 6) Heel Strike as detected via the Metatarsal sensor. 52
Figure 33. Normalized, totaled plantar load data resulting in classic M-curve. 53
Figure 34. Schematic of typical ultrasound transducer (top) and Schematic of transducer with a mutual capacitive pressure sensor (bottom). 59

List of Abbreviations

CDC	Capacitance-to-Digital-Conversion
COP	Center of Pressure
CPU	Central Processing Unit
GPIO	General Purpose Input-Output
HDSA	High Density Count Sensor Arrays
LDSA	Low Density Count Sensor Arrays
PCB	Printed Circuit Board
UART	Universal Asynchronous Receive-Transmit
uC	Microcontroller

Chapter 1 Contributions

This electrical interference as a result of mutual capacitance was popularized in 1919 by Leon Theremin's invention of a musical instrument, the Theremin, which consisted of two antennae (one straight and one loop). These antennae created tone and volume control based on the mutual capacitance detected by the device, as shown in Figure 1. As the player's hand moves closer to the straight antenna, the pitch of the audible sound is modified. The second loop antenna increases volume as the player's hand moves inside or along the edge. In this mutual capacitance phenomenon, the player's hand (or appendage) acts as the ground and completes the circuit. As the player's hand moves toward the antennae, the capacitance increases and sends an analog signal to either the frequency generator or the volume voltage. Since the invention of Theremin this method has been used for general purpose proximity sensing for gesture control in automobiles and location detection in buildings [1, 2], There are also medical applications, including a sensor array on a doctor's lab coat and "go/no-go" on the end of an apparatus or probe to detect contact with the skin [3, 4]. The summary of these efforts with comparable benchmarks is shown in Table 1. This paper evaluates the possibility of utilizing this mutual capacitance phenomenon for pressure sensing, as well as proximity sensing within a single sensor connection.

The transition from sensing proximity to sensing pressure is achieved with the addition of a dielectric layer with known mechanical properties. For example, consider a flat, conductive plate with a layer of rubber over it, and then connected to a circuit with a Capacitive-to-Digital Converter (CDC). As a subject's hand approaches the conductive plate the detected capacitance increases. Once the subject's hand actually presses against the dielectric, there is an initial spike in capacitance as a result of the (mathematical) removal the air's contribution to

the dielectric layers. This initial spike in capacitance is associated with the pressure that is applied to the sensor, exhibiting the first instance of mutual capacitance sensing pressure.\

In a standard Theremin, air acts as the dielectric and does not significantly resist the hand as it moves closer to the antenna. When rubber (or other nonconductive material) is used as the dielectric, the rubber resists the hand and it tries to move closer to the antenna or capacitive plate. The proximity-pressure relationship is a result of the Elastic Modulus of the dielectric is the pressure applied to the surface as determined by the electric potential of the finger via the area and centroid in proximity to the sensor.

This concept is rather direct when investigating relative sensing of proximity and pressure, but quickly becomes complex when absolute proximity and absolute pressure values are desired. The following details the experimental set-up required to configure a mutual capacitive absolute pressure sensor.

Figure 1. Leon Theremin using mutual capacitance to control volume and pitch.

Table 1. Proximity Sensing Benchmarks

Researcher	Method	Conductor Size	Sensing Distance	Capacitance Change	Region Sensing	Proximity Sensing	Pressure Sensing
Buller and Wilson 2006	Capacitance Change in wire	Ø1.6 mm, 36 cm long	< 100 cm	0.2 pF	**YES**	**YES**	NO
Cheng et. al 2008	Gesture Capture	~3 x 5 cm	2 cm	< 50 pF	**YES**	NO	NO
Togura et. al 2009	Gesture Sensing with conductive plate	10 x 10 cm 5 x 5 cm	10 – 40 cm	0 – 0.150 pF	**YES**	**YES**	NO
Palmer 2010	Probe Contact Sensor	~ 2 x 2 cm	Contact	< 50 pF	**YES**	NO	NO
Huber 2012	Conductive plate with dielectric	2.5 x 4.5 cm	3 cm	< 10pF	**YES**	**YES**	**YES**

Section 1.1 Fundamental Contributions

The primary contribution of this project is the creation and application of a single plate and single dielectric capacitance dual proximity and pressure sensor that uses the body's capacitance to act as the ground of the circuit. Conductive surface-to-body capacitance human presence sensing has been attempted for human-sensing for computer interfaces [1], but never as a dual proximity and pressure sensor.

Another primary contribution is the creation of a foil paper that can be cut with a laser, replacing photolithography as an inexpensive, rapid prototyping of a sensor array.

Part 1.1.1 Capacitive Proximity and Pressure Sensing of Human Interaction

Body capacitance presents a fundamental conflict when capacitive pressure sensing is applied to capacitive touchscreens or pedobarography. The body provides 100-150 pF of capacitance [5], which is the fundamental physical phenomenon utilized by capacitive touchscreens [6]. Existing touchscreens do not offer proximity or pressure sensing [6]; the touch location is triangulated from multiple capacitive sensors on the edges of the screen. For pedobarography with a typical capacitive sensor, the capacitance of the foot will interfere with the sensor's capacitance measurement. This can be resolved with additional shielding and, more importantly, added cushion for a greater distance to reduce the foot's capacitive impact to the system. The resulting sensor array is thicker and more rigid than is practical to implement for a flexible sensor for the electronic pedobarographic shoe.

The proposed body capacitance solution is simple, novel, and robust. This concept replaces the traditional ground sensor plate with the body capacitance supplied by the finger or foot, as shown in Figure 2. The sensor consists of a finger or plantar region, dielectric, and capacitive plate. This assembly is the first body capacitive sensor for proximity or pressure sensing.

Figure 3 demonstrates this sensor as a dual proximity and pressure sensor. When the finger moves closer to the capacitive plate the sensor's capacitance value increases, shown as (A) to (B). The capacitance continues to increase until it touches the dielectric on top of the capacitive plate, shown as (B) to (C). The capacitance spikes as the finger touches the dielectric material (C). This spike occurs because the body capacitance no longer passes through the air and dielectric but instead passes only through the dielectric material. At this point, the sensor transitions from proximity sensing to pressure sensing. As the finger presses harder on the dielectric, the responding capacitance increases, shown as (C) to (D) which is correlated to pressure sensing.

This same sensor concept can be applied for pressure sensing the plantar regions of a foot for gait analysis. A typical gait M-curve from a force plate consists of a spike from the heel strike, a dip during mid-stance, and then a spike again during toe lift-off. The foot's position relative to the capacitive sensor through a normal gait is shown in Figure 4. Figure 5 displays the expected sensor response during the gait. For the heel sensor, the sensor spikes during the heel strike then dips as load reduces. During the swing phase, the distance between the heel and the sensor increases and the capacitance begins to increase again as the heel gets into position to strike again. A similar response occurs for the sensor over the metatarsal and big toe plantar regions.

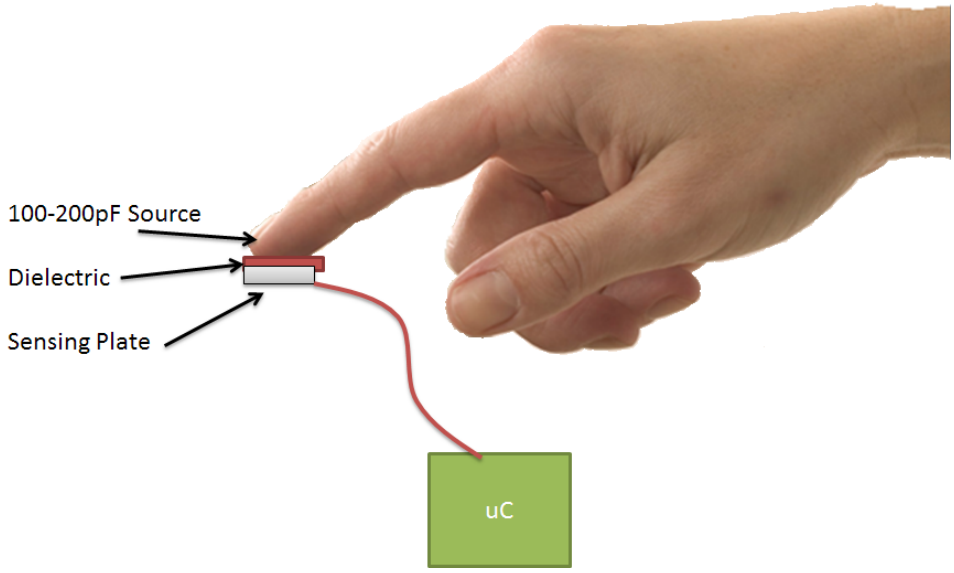

Figure 2. Diagram of the proposed proximity and pressure sensor utilizing body capacitance with a microcontroller to interpret the capacitance values.

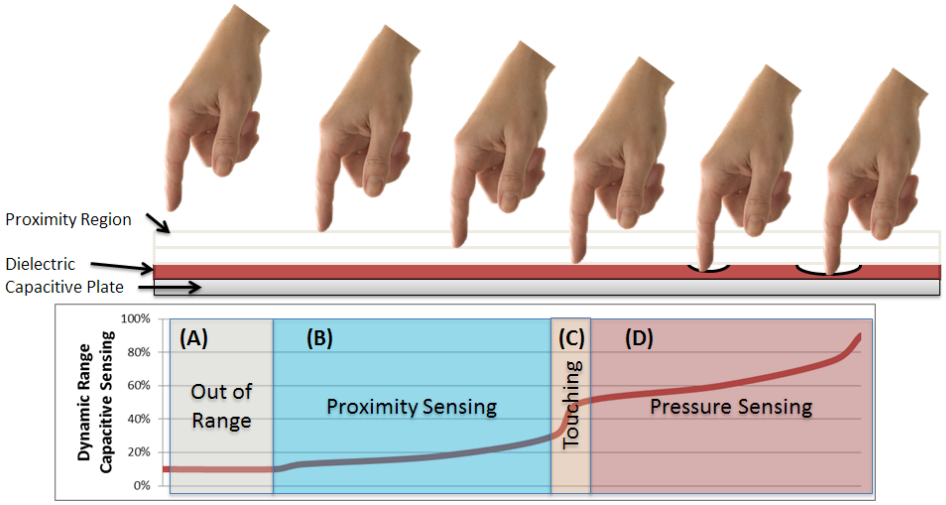

Figure 3. The single capacitive plate used as a proximity and pressure sensor.

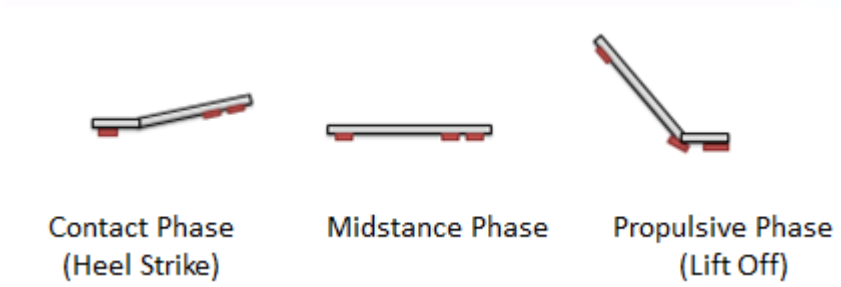

Figure 4. Sensor position inside the shoe through a typical gait.

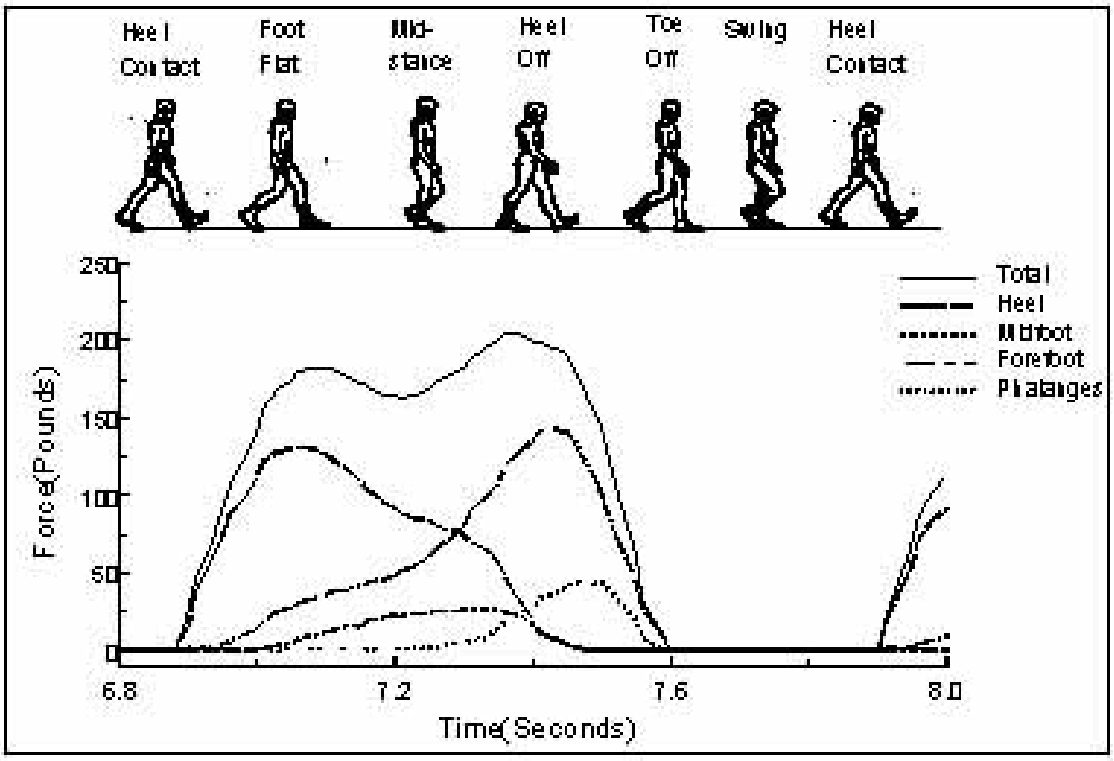

Figure 5. Capacitive sensor response from a typical gait. Image from http://www.med.nyu.edu/rehabengineering/research/locomotion.html

Part 1.1.2 Laser Cut Flexible Sensor

Photolithography sensor fabrication can often take weeks to complete and can have high development costs. While a flexible sensor array was fabricated for this project, the costs and lead-time hinder the rapid development progress. In the lab, hand-cut aluminum foil sensors are used as prototype flexible sensors. While effective, it requires a simplified geometry and is a fabrication method susceptible to human variation. An inexpensive, rapid prototyping solution is needed.

Laser cutting is an obvious choice, but aluminum foil is difficult to laser cut because the surface reflects the laser instead of absorbing it. The proposed solution would be to adhere a layer of paper to a layer of aluminum foil. The material is set on the cutting bed such that the paper faces the laser beam. As the laser cuts the pattern, the paper cuts and causes a shear in the foil which extracts the pattern from the paper-foil material. Now an inexpensive sensor array can be rapidly, repeatable produced. Images from this process from development to prototype are shown in Figure 6.

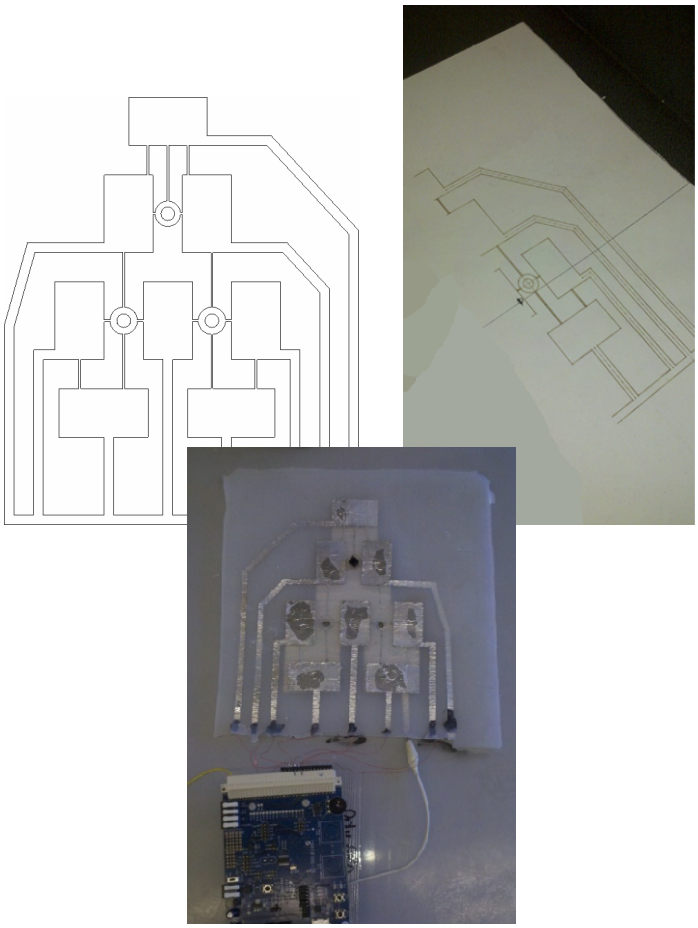

Figure 6. The laser cut sensor process from CAD drawing: to cut, to connection to the microcontroller.

Moving forward within this document Chapter 2 provides the background of previous attempts of utilizing mutual capacitance for proximity sensing as well as previous attempts at gait detection for Pedobarographic studies.

Chapter 3 outlines the hardware setup, sensor options, and software data acquisition.

The results are shown in Chapter 4 with a discussion of those results in Chapter 5.

Chapter 6 then details the possibilities of this technology in the future.

Chapter 2 Background

This chapter starts by reviewing fundamental relationships of a mutual capacitive sensor and builds a set of equations that describes the phenomenon. After that, there is a focus on the previous attempts to apply mutual capacitance as a proximity sensor for human presence, gesturing, and locating an apparatus on a person. These applications are summarized, and then a case study is performed on the development of a Pedobarographic shoe sensor that utilizes the mutual capacitance phenomenon.

The benefit of adding a dielectric layer to the single conductive plate is the dual usage of both proximity and pressure sensing from a single sensor. With respect to the shoe, the sensor detects the distance between the sole of the shoe to the local plantar region. Then as the plantar region initiates contact, the sensor continues to report the capacitance, but now is responding to the applied pressure which thins the dielectric that in turn decreases the distance between the plantar region and the sensor. The result of which is an increase in capacitance.

Section 2.1 Capacitive Proximity and Pressure Sensing Mathematical Relationships

The fundamental equations that define mutual capacitance are simple. However, the relationship between the finger or appendage and the capacitive plate is complex due to the viscoelastic properties of the body. The mutual capacitance is a function of the area of interaction, distance, number of dielectrics, and dielectric coefficients. The number of dielectrics plays a significant role in detecting the difference between sensing proximity and a pressure.

There is another capacitive phenomenon in play with mutual capacitance proximity and pressure sensing. In pure proximity sensing, there are two dielectrics between the finger and the capacitive plate, the elastic material and air. The result is equivalent to the two dielectrics being wired in series, as in Figure 7 [7]. During the transition from proximity to pressure sensing, one dielectric is removed, causing a theoretically instantaneous increase of the capacitive measurement. From this point, the system measures pressure as a result of the increase in capacitance caused by the decrease in distance, which is caused by an increase in applied pressure. While the simplest model of the equations with a perfectly rigid finger show a discontinuity between proximity and pressure sensing, when bulk elastic properties are applied to the finger with small sections of the finger coming in contact with the elastic dielectric, then the model shows a smooth transition with an inflection point as the sensor transitions from proximity to pressure sensing.

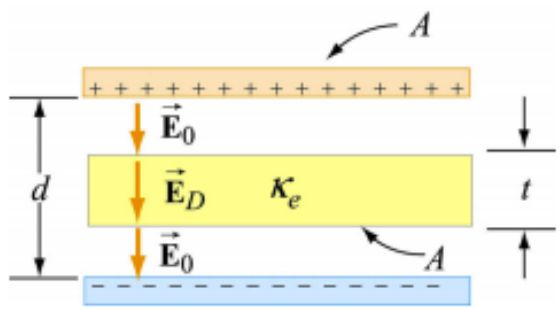

$$\frac{1}{C_{total}} = \frac{1}{C_{air}} + \frac{1}{C_{D1}} + \frac{1}{C_{D2}} + \ldots$$

Figure 7. Diagram and equations exhibiting stacked dielectrics act in series.

Section 2.2 The Pedobarographic Gait Shoe

Pedobarography was introduced by walking across an inked mat in the mid-1920s and has evolved into a complex array of electronic pressure sensors [8, 9]. Today, static and dynamic pedobarographic studies evaluate rheumatoid arthritis [10], congenial clubfoot [11], cavovarus feet in children with Charcot-Marie-Tooth disease [12], and evaluation of diabetic deformities [13]. Additionally, pedobarography is utilized as a post-operative evaluation [14] or to determine the effectiveness of a treatment regimen [15].

Each of these studies measure the foot's pressure distribution during a controlled action or gait to assess the effect of the pressure distribution on a physical condition, or the affect a physical condition has on the pressure distribution.

Part 2.2.1 Center of Pressure Monitoring

Center of pressure (COP) is the center point of the pressure distribution of the foot to the ground forces and can be associated with a static or a dynamic pressure pattern [16]. Tracking COP has become the primary analysis technique for numerous pedobarographic studies [17], including shifts in gait COP of a diabetic foot compared to the control group [16], determination of a patient's muscle strength regime to improve dynamic balance in patients with knee osteoarthritis [18], and determination of walking pressures in young and mature adults [19].

While the previously mentioned studies demonstrate the diverse functions of COP analysis, Kul-Panza provides a strong endorsement for the need of correlating pedobarography

and knee health. He concluded that, "pedobarography may become a useful technique to determine foot pressures that change because of disturbed weight-bearing and balance problems in knee osteoarthritis." For his study, the pedobarographic data from a walking gait was compared with the ability to maintain balance in patients with knee osteoarthritis [20]. The study determined pressure in the hindfoot and peak pressure were lower in the osteoarthritis group compared to the control. Also, the sway width while balancing was higher in the osteoarthritis group.

Part 2.2.2 Electronic On-Shoe Pedobarography

Flex-Force is an eight sensor array that measures plantar foot pressure as resistance [21]. The sensor has been tested to 100 N which results in 1000 kPa by applying force in steps of 10 N and constant speed of 0.1 mm/min. During an orthotic study, the initial results indicate applied pressures in range of 50 to 400 kPa for a normal subject and higher pressures (greater than 600 kPa) at metatarsal heads for diabetic patients.

A gyroscopic gait detection system has shown promising results [22]. It is able to predict gait with 99% accuracy during walking on flat, irregular, and inclined surfaces. When the patient is impaired, the system is 96% accurate. The sensor signals are sampled at a frequency of 100 Hz with a resolution of 10 bits and processed on a 20 MHz microcontroller board. The system detects a 3° change in heel rotation.

The GaitShoe [9] is a gait analysis system that can retrofit into a patient's shoe [9] permitting the shoe to transmit data wirelessly. The GaitShoe prototype runs from a 9 Volt battery and weights 200 grams. The device contains gyroscopes, accelerometers, sonar, and force sensitive resistors. This development group has not determined an analytical method for

processing the acquired data, such as the sensor output from a five second walk into meaningful pedobarographic characteristics.

Fullen systems holds a patent on a sensor array consisting of a conductive material between two electrodes [23].. This insole system reads and computes pressure signals within the shoe. When a pressure is detected above a specified threshold, the circuit triggers a sound to notify the wearer of the increase in stresses.

Polodoff and Tekscan hold a patent on a sensor array consisting of two layers of intersecting electrodes and a pressure sensitive resistive material in the middles [24]. This device is the mainstream selection for electronic pedobarography.

Table 2. Summary of gait detection methods and sensor location

Year	Who	Force Sensing Type	Gyroscope	Sensor Count	Method
1991	TekScan	Piezoresistive	No	256	Contact on the bottom of foot
1994	Fullen Systems	Conductance	No	256	Contact on the bottom of foot
1999	Novell	Piezoresistive	No	200	Contact on the bottom of foot
2001	Pappas	Piezoresistive	Yes	3	On outer, bottom of the sole
2008	GaitShoe	Piezoresistive	Yes	4	On outer, bottom of the sole
2009	ForceFlex	Piezoresistive	No	256	Contact on the bottom of the foot.
2012	Huber	Mutual Capacitive Proximity and Pressure Sensing	No	3	Contact on the bottom of foot at plantar region

Part 2.2.3 Design Objectives for Capacitive Shoe Insole Sensor

Most studies discussed earlier utilized high-density count sensor arrays (HDSA) consisting of 200-1000 sensors per foot. The recent attempts in On-Shoe Pedobarography reduce that count by placing a small number of pressure sensors at specific regions of interest. While the sensor resolution is reduced, the information from these devices still provides useful pedobarographic feedback to the researcher. One drawback to the design of lower density sensor arrays (LDSA) is sensor placement. HDSA systems create the regions of interest via software analysis; whereas, the LDSA designs must custom fit the sensor placement per patient to ensure accurate experimental data.

Pedobarographic technology is progressing toward requiring fewer strategically placed sensors, there are few suggestions for this trend:

- Improved dynamic response with fewer sensors.
- Reduced manufacturing cost with some sacrifice of data accuracy.
- Less data to transmit wirelessly with LDSA.

It should also be mentioned that LDSA are being designed for specific applications, whereas, HDSA are purposed for a wide range of functionality to a general audience.

This is also the first plantar region specific approach to sensing. The ForceFlex sensor array from TekScan was used to demonstrate that the instead of a sensor array, strategically placed sensors under the plantar regions provide sufficient sensing for plantar pressures [21].

Chapter 3 Design and Methods

This experimental set-up for palpation proximity and pressure sensing integrates a baseline force sensor (TekScan FlexForce) as the control, a capacitive plate, a dielectric, and a Silicon Labs C8051996 Demoboard CDC with UART communication-to-data acquisition software.

The purpose of the set-up is to create third data relationship. First, the Elastic Modulus of the material must be determined. Dependent upon desired precision, this value can be attained using generic material properties, or the stress-strain data can be collected via an Instron. Secondly, spacers of a known thickness were placed over the capacitive sensor which revealed the proximity-to-capacitive relationship (of more value to palpation sensing than gait detection). Thirdly, the capacitive sensor must be electrically isolated and resting on another pressure sensor. The sensor transitions from proximity to pressure sensing once the baseline pressure sensor begins registering an applied pressure. Figure 8 represents the data connections from this set-up.

The resulting system creates a deflection-CDC counts proximity-pressure- to-capacitance relationship. All of these components are necessary for a successful absolute proximity and pressure sensor, and it is unnecessary that the capacitance-to-counts ratio be known. Counts become the conversion that connects force to deflection. One can perform calibration using known capacitors to generate a custom reference table and determine the counts-to-capacitance relationship.

This project utilized a Silicon Labs C8051F996 microcontroller. This chip supports 14-port CDC at 25 kHz with UART communication to the data acquisition software. Additionally, this chip can span to a virtually unlimited number of sensors in an array based on a combination

of Master-In-Slave-Out (MISO) parallel processors and multiplexors. For this evaluation, the onboard 14-ports were sufficient.

The mutual capacitive effect is detailed in Figure 9. The detected capacitance has a gentle increase as the user gets closer until the point when the user is close enough to the dielectric such that a rapid increase in capacitance is detected. All capacitive increases from this point are from pressure sensing. The standard set-up for palpation sensing consists of a capacitive plate and a dielectric material, as shown in Figure 10. The test set-up was used to characterize proximity mutual capacitance for one finger, two fingers, and the palm of a hand. Three replicates of each type were collected with hard stops placed at 4.35mm increments with proximity data collected between 6.35 and 25.4mm. The sensing distance for the dia12mm sensor was 25.4mm. It should be noted that larger sensors allow for a larger sensing distance [2].

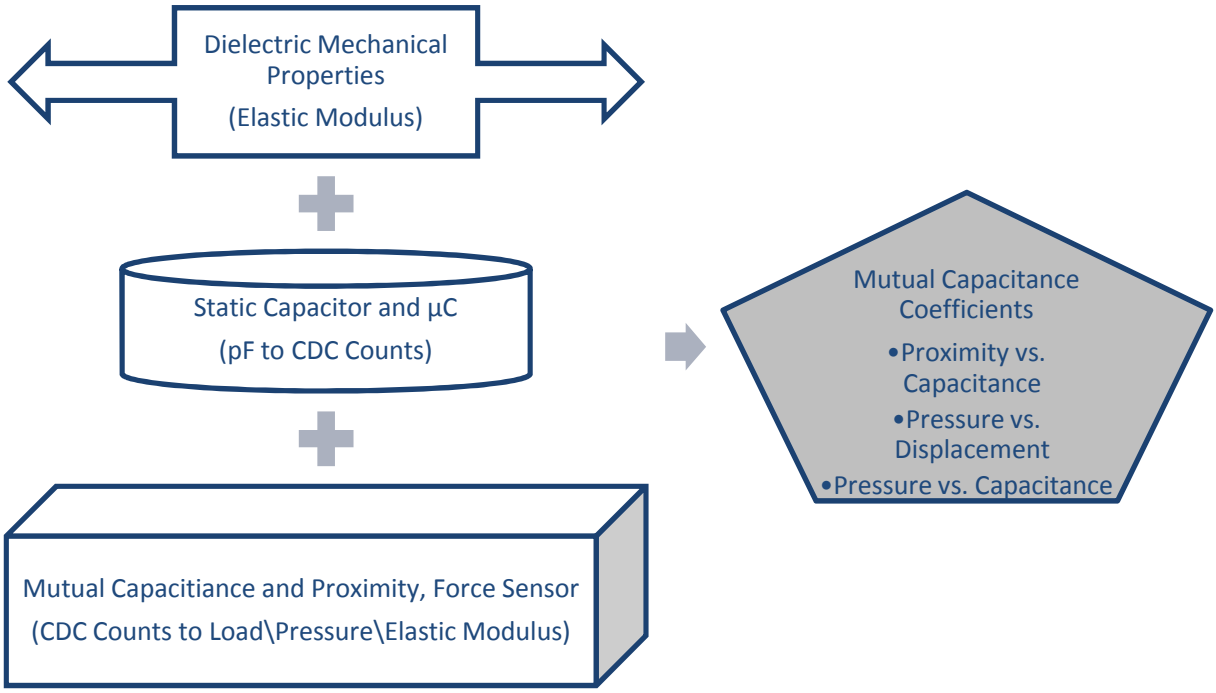

Figure 8. Process to convert a relative proximity and pressure sensor into an absolute sensor.

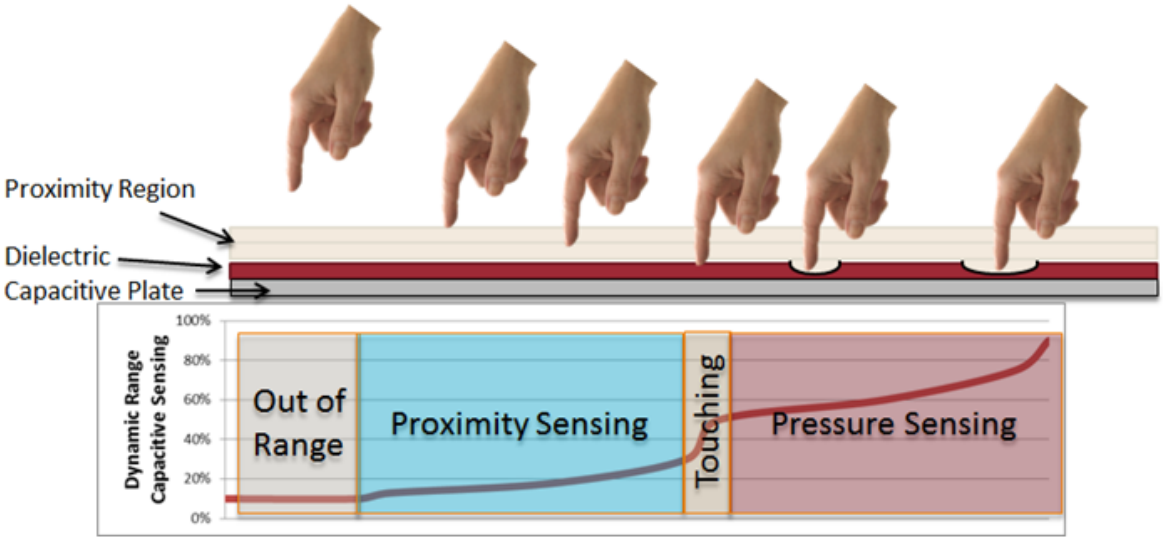

Figure 9. The fundamental concept of mutual capacitance proximity and pressure sensing.

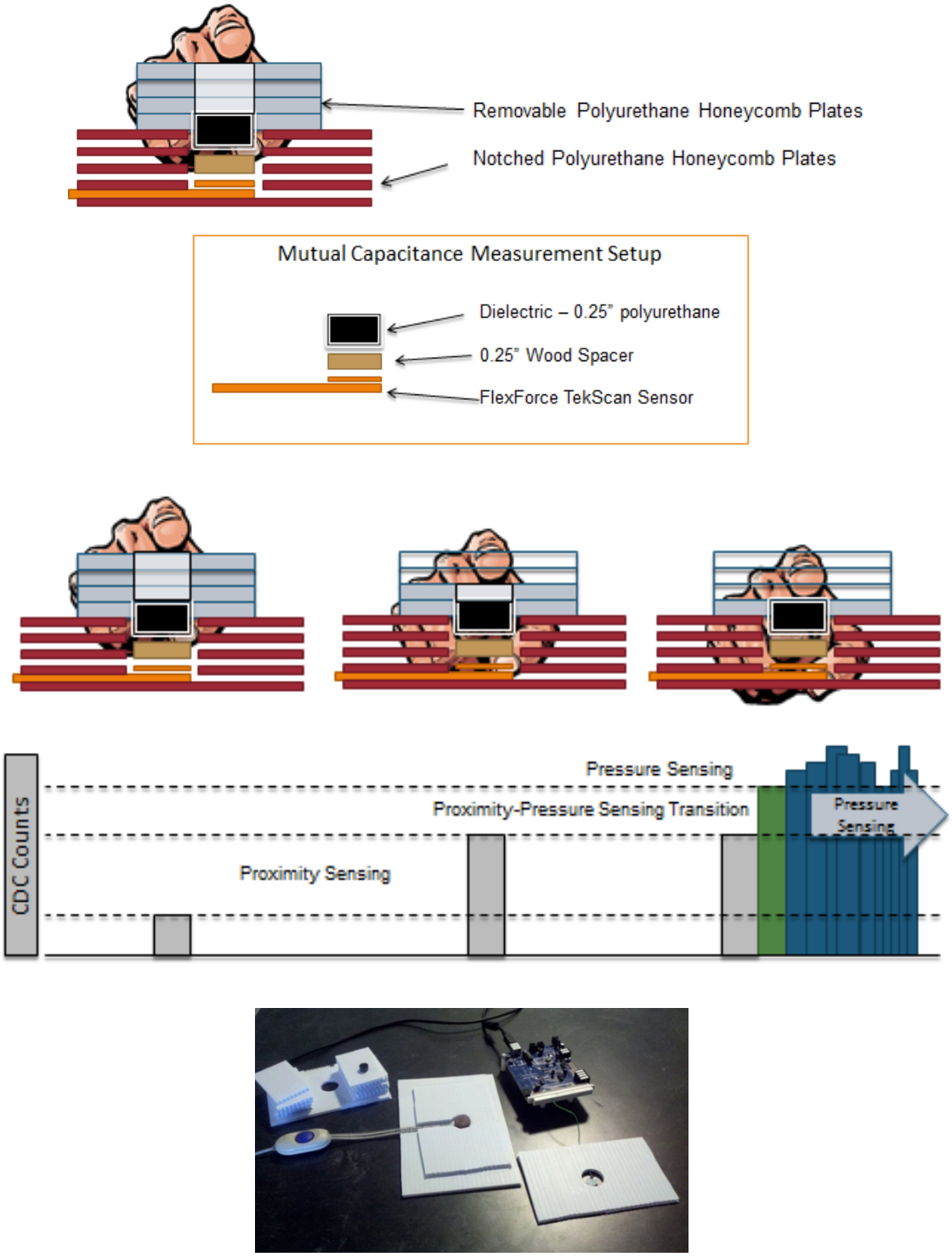

Figure 10. Test set-up to establish fixed proximity points and subsequent transition to pressure sensing.

Section 3.1 Controller Hardware

The system's ability to rapidly perform a Capacitance-to-Digital Conversion (CDC) is paramount to promptly report the applied force over a specific sensor region. During review of currently available CDC technology, one microcontroller (uC) stood alone: the SiLabs C8051F966, which combines general uC functionality (GPIO, UART, MISO, JTAG\C2 Interface) with specialized CDC functionality:

- 14-ports available for CDC
- 12-bit, 25 kHz CDC sample rate
- Internal oversampling for noise reduction and bandwidth control

Having 14 ports available for either GPIO or CDC allows for numerous combinations of uC, MUX, and MISO solutions. Section C-4 of this chapter outlines these options during the discussion of sensor fabrication options. The CDC sample rate is critical in determining the overall sensor array frame rate. Finally, the uC's ability to oversample performs all noise reduction on the uC, reducing the volume of data to be transmitted and simultaneously reducing the PC's CPU load to perform real-time calculations.

An evaluation of this microcontroller's capacitance calculation accuracy is included in Appendix A, as well as the required source code to perform various functions outlined in this document. In general, the 12-bit output matched a linear regression of at least 95% across all gain settings.

For MUX applications, the uC's GPIO ports are configured to digital and communicates with the MUX as specified by its truth table. The uC has a 5 kHz digital on\off switch, that is 20 ms.

Part 3.1.1 Single Microcontroller with CDC

This basic hardware configuration utilizes the 14 available ports for capacitance conversion. When this microcontroller is packaged within its demoboard (as in Figure 11), it becomes a very simple development platform to evaluate many different proximity and pressure sensing concepts.

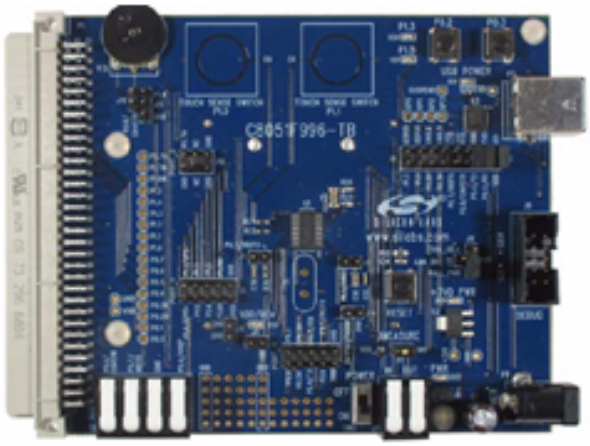

Figure 11. Silicon Labs C8051F996 microcontroller [25]

Part 3.1.2 Multi-MicroController MISO Connectivity

The Master In-Slave Out features of the SiLabs microcontroller become useful when greater than 12 ports of CDC are required, and the sampling rate needs to be faster than 200 Hz and up to 25 kHz. This design requires one microcontroller to act as the master and up to 12 other microcontrollers to connect as slaves, as shown in Figure 12. The result is a maximum of 120 ports that can collect data at rates up to 25 kHz. The master printed circuit board is shown in Figure 13.

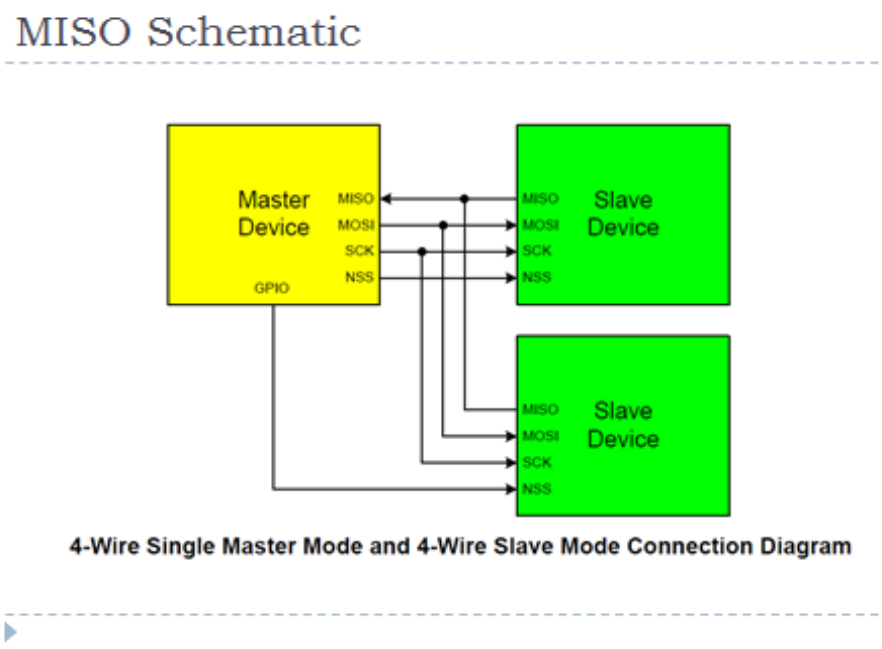

Figure 12. Basic MISO schematic

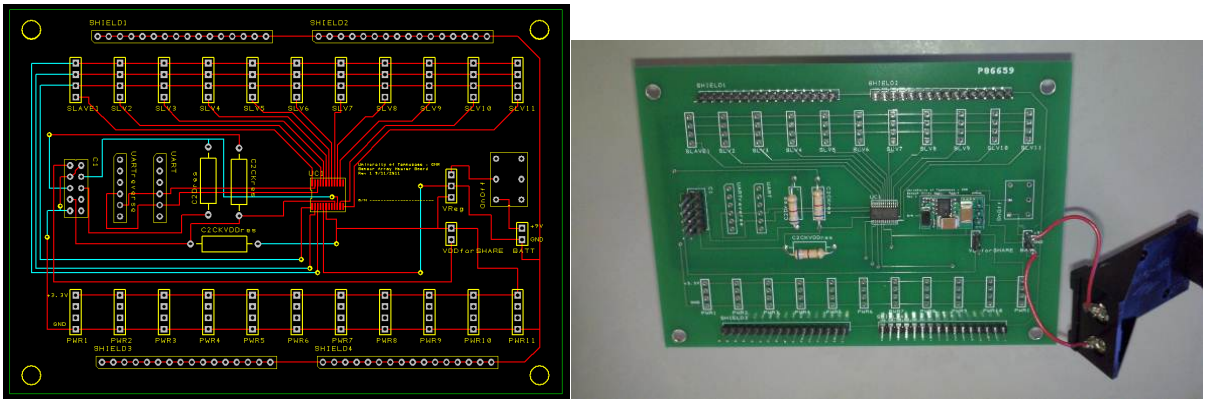

Figure 13. MISO Master PCB: concept and fabrication

Part 3.1.3 Multiplexor PCB with MicroController

This design replaces the 12 slave microcontrollers with two multiplexors. While the hardware schematic is simpler to implement, this comes at the penalty of sampling rate. The microcontroller and multiplexor PCB is shown in Figure 14. It was anticipated that more microcontrollers can read more sensing plates simultaneously, although the switching time of the microcontroller when controlling the multiplexors was unexpected. For the microcontroller to control the multiplexor, it must send a digital logic signal based on the multiplexor's truth table. The microcontroller switches digital logic at 5000 Hz. This switching rate limits the sampling rate of the sensor array. The result limits a 256 count sensor array (16 x 16 multiplexors) to a 0.05 Hz sampling rate. This rate becomes prohibitive for fast response applications.

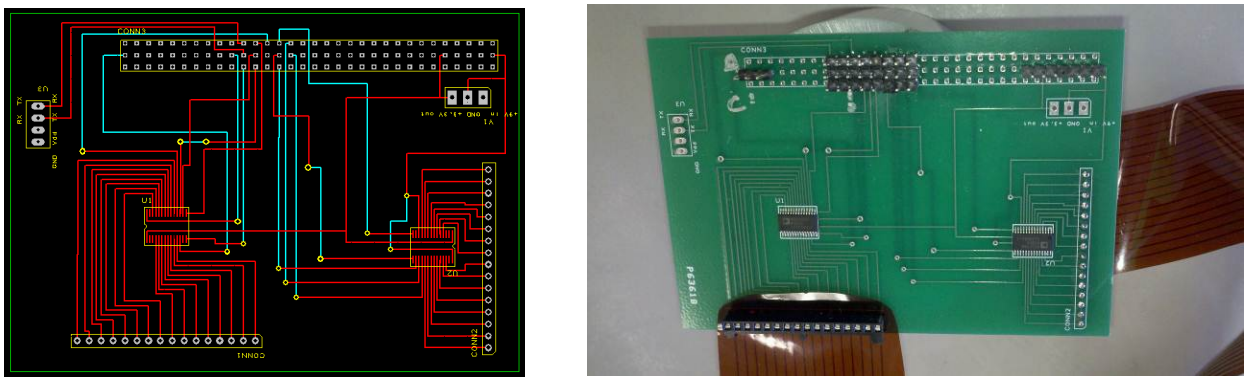

Figure 14. Sensor array PCB for multiplexor

Section 3.2 Selection of Sensor Dielectric Material

Both of these materials have pivitol roles to play in designing a successful pressure sensor with a sufficient dynamic range for the specified application. The dielectric material's elastic modulus determines the change in distance between the sensor plates, which drives the change in capacitance, whereas sensor fabrication determines the geometry of the sensing region and the development costs.

The type of dielectric material directly depends on the application of the sensor. For the pedobarographic shoe, the dielectric needs to be able to have a linear compression between 0-900 pounds on an individual sensor. This maximum load is determined by a 300 pound person with a impact magification of 3. This set of specifactions allows for a sufficient dynamic range for a heel strike impact during a typical walking gait. For the breast phantom, the maximum

sensing load is under 10 pounds. Here, a soft material is preferred to allow for larger deflections, improving the dynamic range of the sensor.

Various dielectric materials were tested by 'sandwiching' two aluminum foil sensor plates around a dielectric material and connected to the microcontroller. The sensor assembly was then placed inside of a compression Instron capable of providing a load of 1000 N. A stress-strain curve and a capacitance-deflection curve were created for each material listed in Table 3. After test conclusion, it was determined that neoprene would be the optimal material for pedobarographic sensing because it was fairly stiff, and yet provides a good sensing range. For the breast phantom, both polyurethane and Dragon Skin gels were soft enough to be sensitive to light, intermediate, and deep palpations. A sample calculation using polyurethane is shown in Figure 15 with Capacitiance to Load and Counts to Load in Figure 16. There was an initial compression of the foil to the dielectric and then the sensor begins to act repeatible. Neoprene was selected for the plantar shoe sensor and Polyuerthane for the Palpation sensor. These applications span 0-300lb loads for gait detection and just 0-3 pound loads for palpation sensing.

Table 3. List of dielectric properties

Sensor Application	Material	Hardness (OO)	Elastic Modulus (MPa)	Thickness (inch)
Plantar Region Shoe Sensor	Neoprene	90	71	0.125in
Plantar Region Shoe Sensor	Natural Gum Rubber	50	58	0.125in
Plantar Region Shoe Sensor	Latex	60	65	0.062in
Medical Phantom Sensors	Polyurethane	30	2.0	0.25 in
Medical Phantom Sensors	Smooth-On Skin	20-40	1.7-2.0	Cast (~0.25in)
Medical Phantom Sensors	Q-Gel	20-30	2.0	Cast (~2in)

Testing Sample

$\varepsilon_o = 8.854 \times 10^{-12}$ F m^{-1}
$\varepsilon_r = 3.5$ MV at 1 kHz
$A_{int} = 0.5$ in^2
$d_o = 0.25$ in
$E = 1.986$ MPa

$$C = \frac{\varepsilon_0 \varepsilon_r A_{\text{int}}}{d_0}$$

$$\Delta d = d_0 - d_1$$

$$\Delta d = d\varepsilon_z$$

$$\sigma\varepsilon = E$$

$$\varepsilon_z = E / \sigma_z$$

$$\Delta C = \frac{\varepsilon_0 \varepsilon_r A_{\text{int}}}{d(E / \sigma_z)}$$

Figure 15. General Capacitive equations as a ratio of electric potential strain to mechanical strain. Data collected for Polyurethane shown.

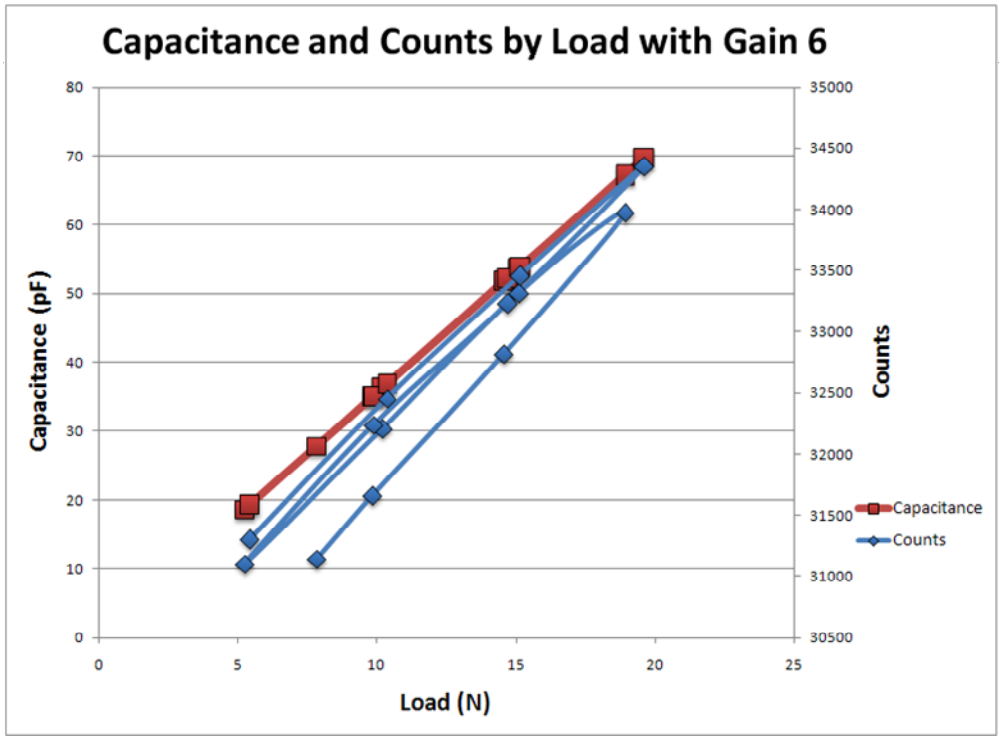

Figure 16. Cyclic loading of capacitive sensor during Instron compression testing.

Section 3.3 Sensor Fabrication Methods

Creation of a capacitive pressure sensor requires two regions of conducting material separated by a dielectric. Sensing regions can be fabricated by cutting the shapes using scissors, transferring a pattern into a circuit with lithography, or laser-cutting a shape in the conductive material. These fabrication methods were evaluated for flexibility, dynamic range, ease of system integration, cost, and fabrication time.

Part 3.3.1 Simple Copper Plates and PCB Etchant

A simple dual copper plate array was designed and assembled, consisting of numerous, random sensor sizes, to read a multiplexor sensor array, whereby the SiLabs C8051F996 microcontroller was officially selected. This non-uniform sensor size helped confirm the multiplexor sensor's switching was occurring properly and helped determine the capacitance drift between the first sensor and the last sensor in the array.

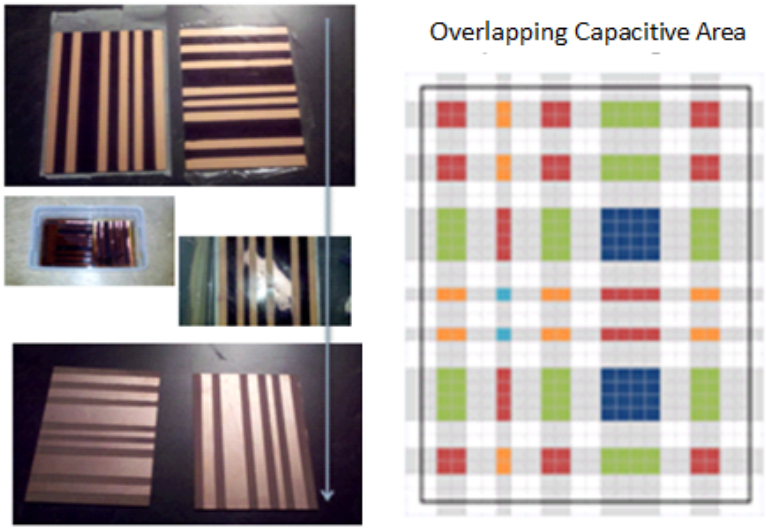

Figure 17. Test setup to evaluate C8051F996 mircocontroller's ability to perform CDC array sensing with a multiplexor.

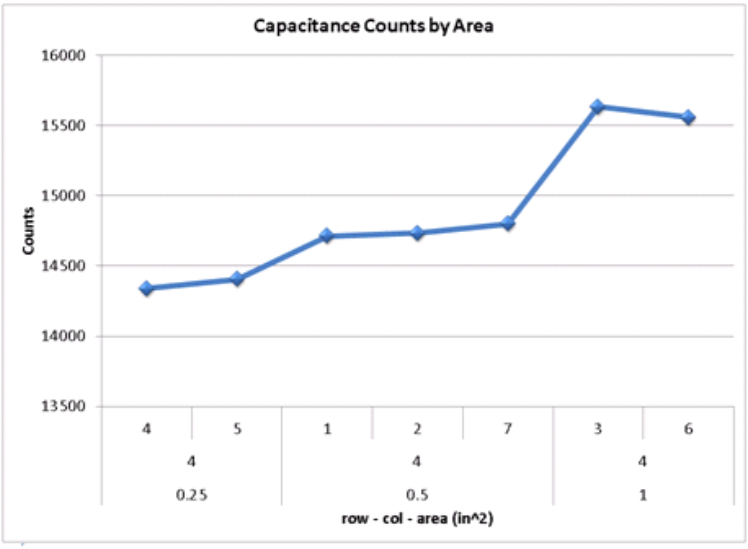

Figure 18. Sensor row number, column number, and sensor's overlapping area. The microcontroller is compatible with multiplexor array sensing.

Part 3.3.2 Lithography Flexible Sensor

After the simple copper plate design comfirmed that the microcontroller was capable of reading individual sensors in the array, the next step was to incorporate a flexible design (design process flow is shown in Figure 19). In order to meet a wide range of applications (i.e., from shoe sensor to breast phantom), the sensor array needed to be modular, so various materials could function as the dielectric for each application.

AllFlex, Inc. (Salt Lake City, Utah) provided the ideal fabrication solution to meet the assorted applications for which the sensor array would be used, as the manufacturer was capable of fabricating 18x24 inch flexibile sheets. Typically, the manufacturer fabricates a single pattern in an array over the entire sheet, but for this project, AllFlex, Inc. layed out numerous sensor geometries onto the sheet, permitting a single manufacturing print to be applied to numerous applications. Likewise, the print maintained the necessary modularity with regards to the dielectric type, allowing various materials to be incorporated according to the application's needs. The final design is 2mil copper surrounded by 5 mil of polyester, shown in Figure 20.

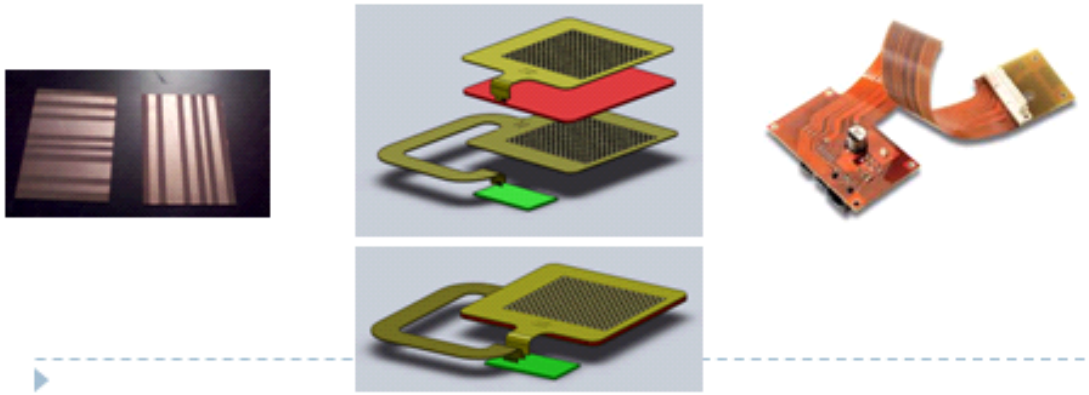

Figure 19. Design strategy for flexible sensor array

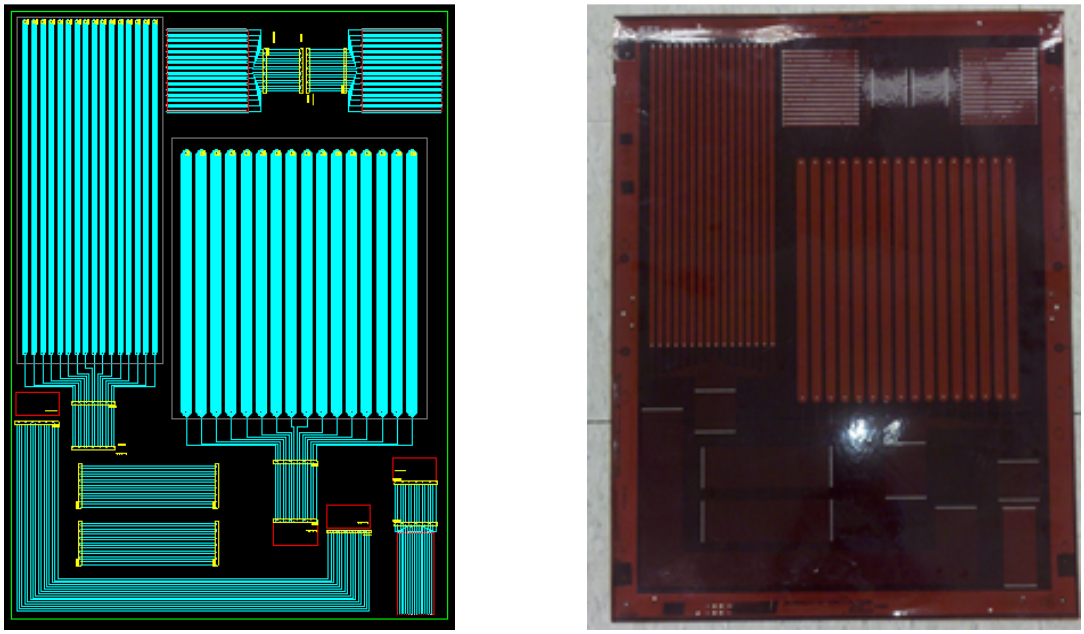

Figure 20. Flexible sensor array design and fabrication

Part 3.3.3 Laser-Cut Aluminum Foil Sensor Array

Ultimately, the photolithography sensor array was determined to be the final design, but an evaluation of laser-cut sensor arrays was conducted between concept and final design. This prototyping method allows for repeatable fabrication while keeping development time and costs at a minimum. The cost and lead-time comparison is shown in Table 4. Laser cutting foil is the quickest, most cost effective method to rapidly prototype a reproducible sensor for testing.

Traditional attempts at laser-cutting aluminum foil have been unsuccessful because of the foil's reflectivity, wherein the laser reflects off the foil instead of residing in the membrane of the material, building heat to initiate a cut. For this concept, aluminum foil and paper are joined with an adhesive layer. The laser then makes contact with the paper and builds heat in the foil, resulting in a heat-shear in the foil.

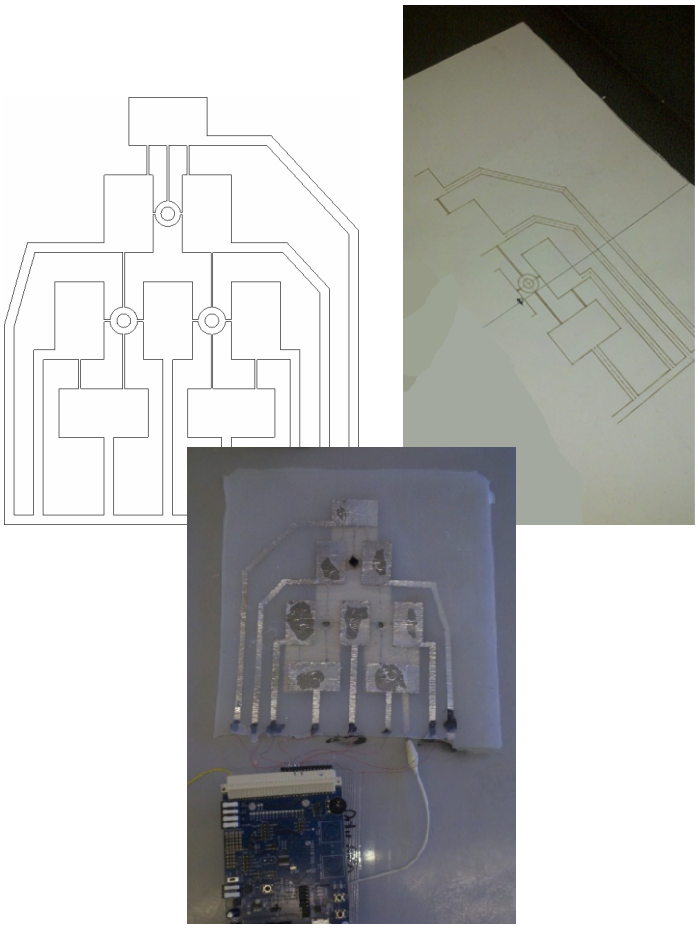

Figure 21. The laser-cut sensor process: CAD drawing, cutting, and connecting to microcontroller

Table 4. Comparison of sensor array fabrication methods

Sensor Fabrication	Flexible Sensor	Modular	Minimum Feature Size	Manufacturing Time	Manufacturing Cost
Copper Plates and PCB Etchant	No	Yes	5mm	1 day	$10
Photolithography Copper and Polyester	Yes	Yes	5 micron	6 weeks	$800 tooling charge per concept. $1000 per sheet
Laser Cut Aluminum Foil and Paper	Yes	Yes	1mm	5 minute paper assembly 5 minute cut	<$1 per sheet for materials $20 per sheet to laser cut

Section 3.4 Data Analysis

Part 3.4.1 Data Acquisition Graphical User Interface (GUI) and Real-time Display

Data collection, visualization, and subsequent analysis are essential and for a significant number of applications, the visualization and analysis are performed in a post-processing environment. However, this paper aims to understand the effect of visualization and analysis in a real-time environment. The computer is simultaneously responsible for data collection, visualization, and analysis which results in a higher central processing unit (CPU) burden.

Two Biomedical Engineering Design teams from the University of Tennessee have recently developed pressure sensor systems: a shoe sensor used for gait prediction and a rib cage to determine palpation force and location during a breast exam. In the case of these projects, the visual feedback and the predictions must be performed in real-time to aid the software operator to make immediate assessments.

Part 3.4.2 Method

The following addresses the test plan for evaluation, as well as compare frame rates:

I. Universal Asynchronous Receiver/Transmitter (UART) Data
   a. Data collection constant stream
   b. Data collection constant burst
II. Data collection with Real-time Visual Feedback in Matlab
   a. Bar Chart
   b. Surface Plots
   c. Image Plots
III. Data collection with Decision Making
   a. Threshold detection
   b. Data collection with Real-time Visual Feedback and Decision Making

Figure 22 shows the program utilized to collect the UART data. It contains Connect\Disconnect buttons, a data display window (bar chart shown), real-time raw data display (High and Low bit), and data points per loop. The value entered for data points per loop drives the frame rate of the interface by specifying the number of data points before the screen refreshes. During one loop, the program is expected to collect the data packet, process the incoming data, make a prediction or decision based on the incoming data, and then display both the data and prediction. This program flow is shown in Figure 23.

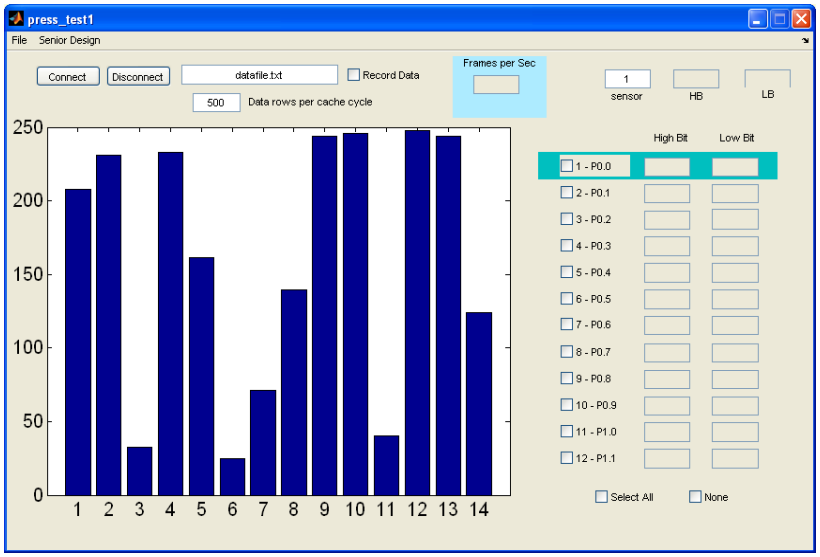

Figure 22. Sensor data collection GUI

Figure 23. Sensor data collection program flow

Part 3.4.3 Data Acquisition Results

A graph of data point results for various run conditions is shown in Figure 24. Data collection frame rates. Matlab was able to collect and process considerably faster when the graphics were not activated. When the graphics were activated, the surface maps were the fastest method, followed by image generation, then drawing a bar chart. Although, the values were close enough that a particular application may create different results.

Figure 25 reveals the examination of each situation, given 100 data points per loop. The baseline data collection with decision making occurs at 40 frames per second. Activating the High and Low bit raw data costs 10 frames. Activating the graphics costs approximately 20 frames. However, activating both features costs 25 frames per second.

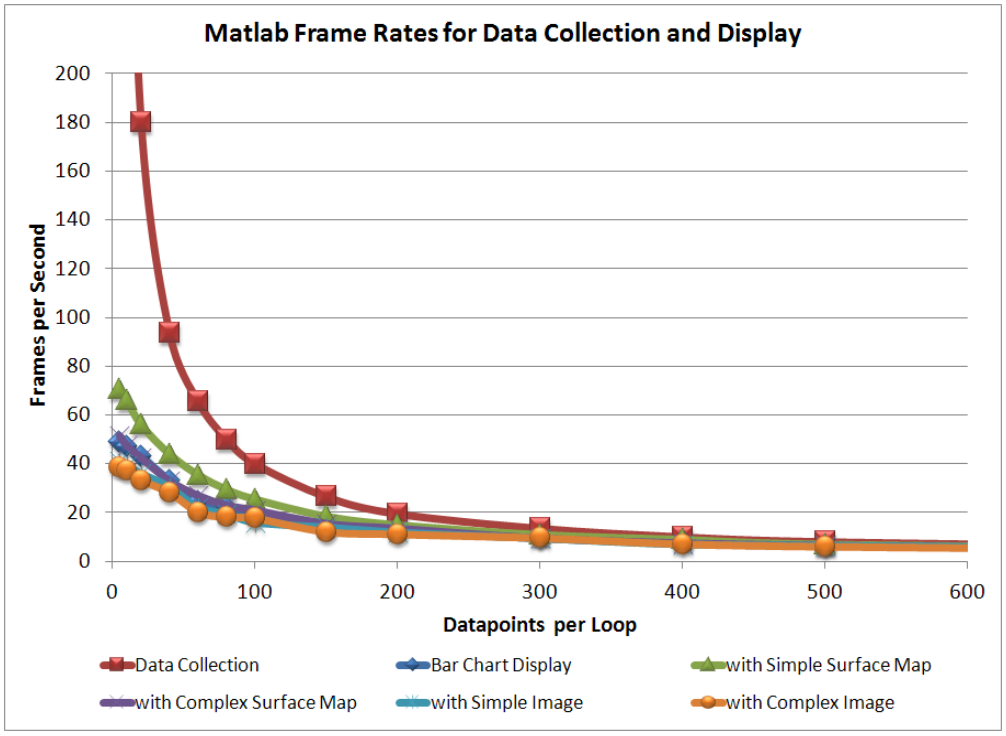

Figure 24. Data collection frame rates

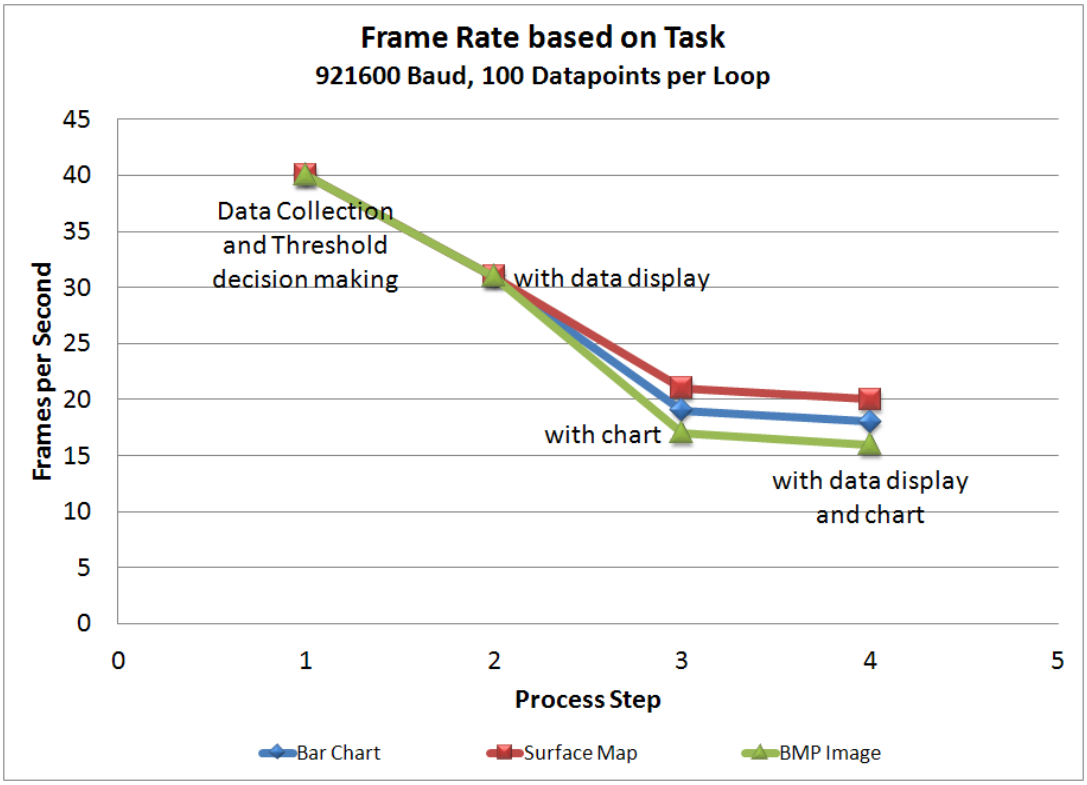

Figure 25. Data collection frame rates per specific function

Part 3.4.4 Summary of Data Acquisition and GUI Frame Rates

Matlab is capable of capturing an UART datastream and performing some analysis on that data faster than the data is received. However, Matlab has demonstrated a significant CPU load when trying to refresh the visualization of the data. This CPU load was observed using the built-in functionality of bar and surface plots and the creation of a bitmap and then drawing the image. Each case shows a 50% drop in frame rates when the data visualization is enabled.

Chapter 4 Results

Section 4.1 Palpation Proximity and Pressure Sensing Results

Proximity sensing sensitivity data was collected one finger, two fingers, and the palm of a hand approaching a 0.5 inch diameter aluminum foil sensor with a 0.5 inch diameter polyurethane dielectric on top of it. Figure 26 shows that there was little proximity difference between one and two fingers. The mutual capacitance of the palm of the hand becomes significantly different from the fingers at 0.4 inches from the sensor. At the final layer, the palm is cupped over the sensor resulting in a large increase in perceived proximity. This sensor can detect ±100 counts if the appendage is unknown. Meaning that the software is not expecting one finger, two fingers, palm, or whatever the desired interface. This range results in a calculated ±0.205 inches (5.2mm) of error. If the interfacing appendage is known, then the accuracy improves to ±25 counts. Now, the sensor is accurate to within ±0.051 inches (1.3mm).

Pressure sensing for a single finger pressing on the described setup was collected and is shown in Figure 27. The TekScan FlexForce sensor data is shown on top and CDC counts data shown on the bottom. The counts show an increase as the digit approaches the sensor. This is the proximity region. The finger is the pressed hard (3000g) against the dielectric and sensor followed by four softer (700 grams) presses. From the data shown in Figure 27, this system was capable of detecting applied load to ±250 counts which translates to ±400 grams (0.88 pounds). Also, taking data from the dielectric compression tests sensor is detecting ±0.020 inches (0.5mm) proximity detection via the compression of the dielectric material.

This data is summarized in Figure 28. It represents the flow of data to process an absolute mutual capacitive proximity and pressure sensor instead of a relative sensor.

This microcontroller was tested with 10 50 pF static capacitors connected in series and parallel, resulting in a range of 25 – 200 pF at various gain settings; the signal-to-noise ratio (SNR) ranged from 200 to 1500. The Rose criterion states that an SNR of at least five is necessary to be capable of distinguishing image features with 100% certainty. Hence, the microcontroller will provide accurate, reliable results consistent with the expectations of a commercially available mass-produced device.

Using three trials of palpation proximity sensing with the test set-up demonstrated a sensing sensitivity of +/- 25 and 100 counts, dependent upon whether or not the appendage was known. This count range results in +/-1.3 and 5.2 mm of error. Mutual capacitive pressure sensing with a dielectric demonstrates a +/- 250 counts variation (+/- 1 High Bit of 12 bits), which corresponds to +/- 3.9 Newtons. This error can be traced back to proximity with the Elastic Modulus of the dielectric (polyurethane in this case). The corresponding deflection is +/- 0.5 mm.

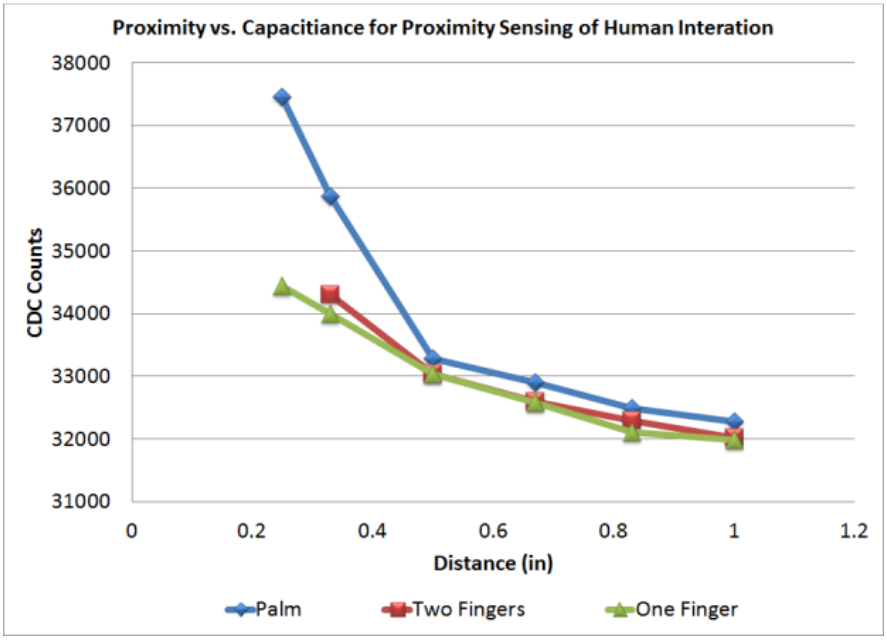

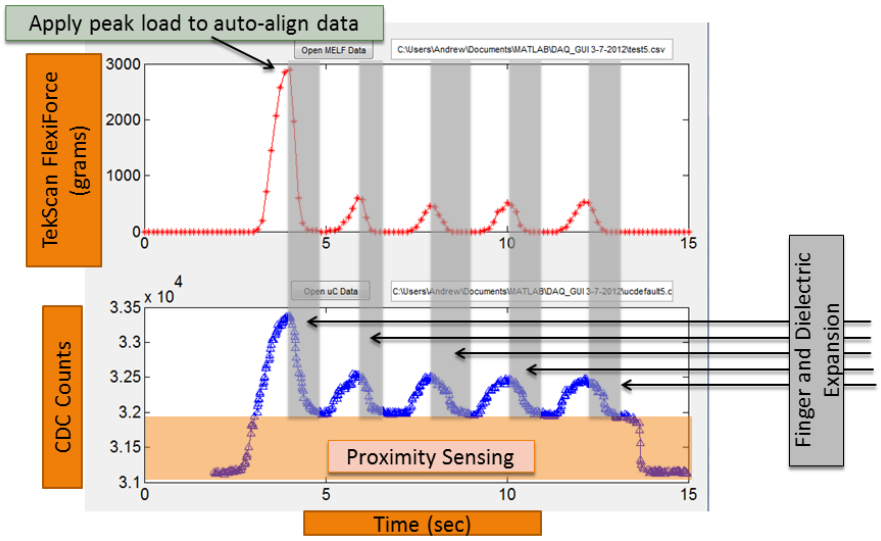

Figure 26. Mutual capacitance increase of a finger approaching a dielectric and capacitive plate.

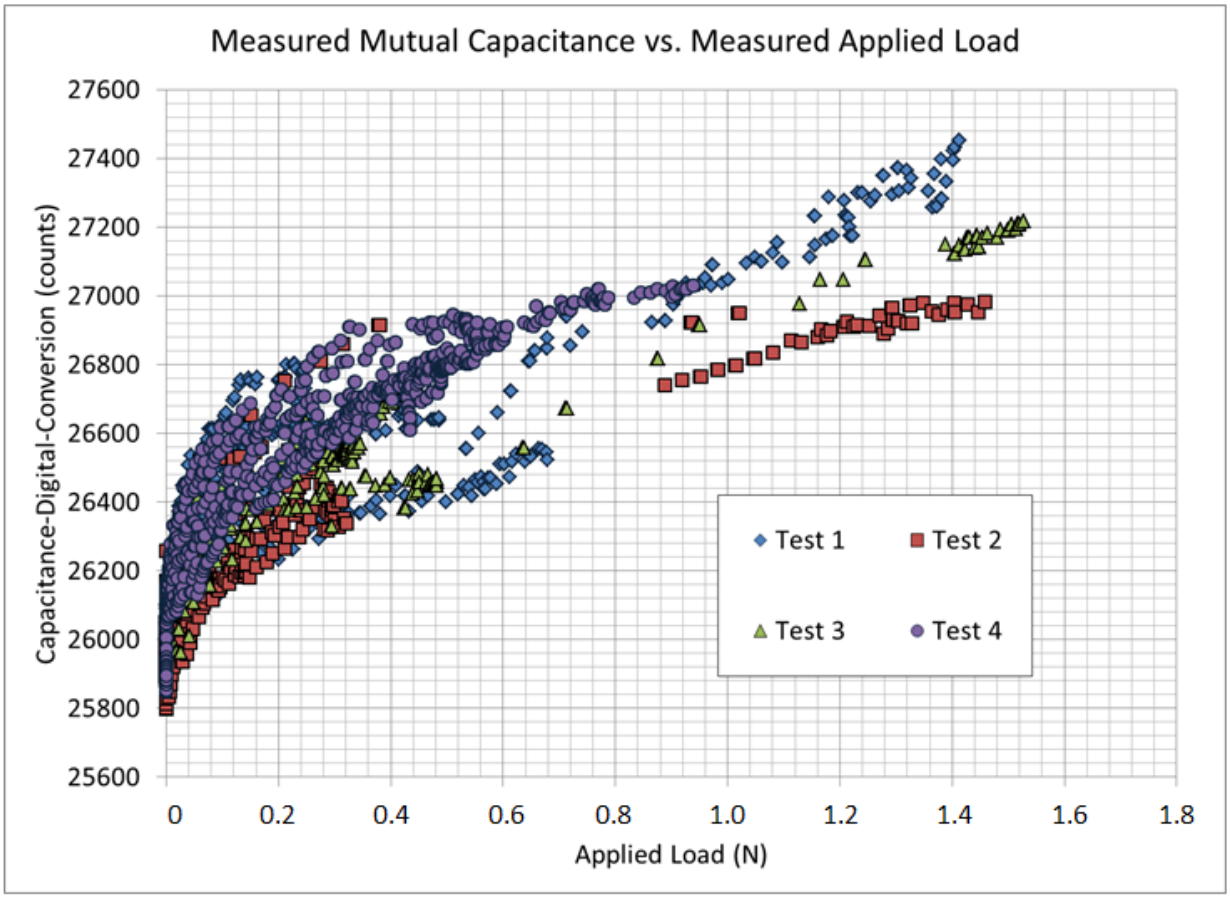

Figure 27. Pressure sensing tests for CDC counts-to-load relationship.

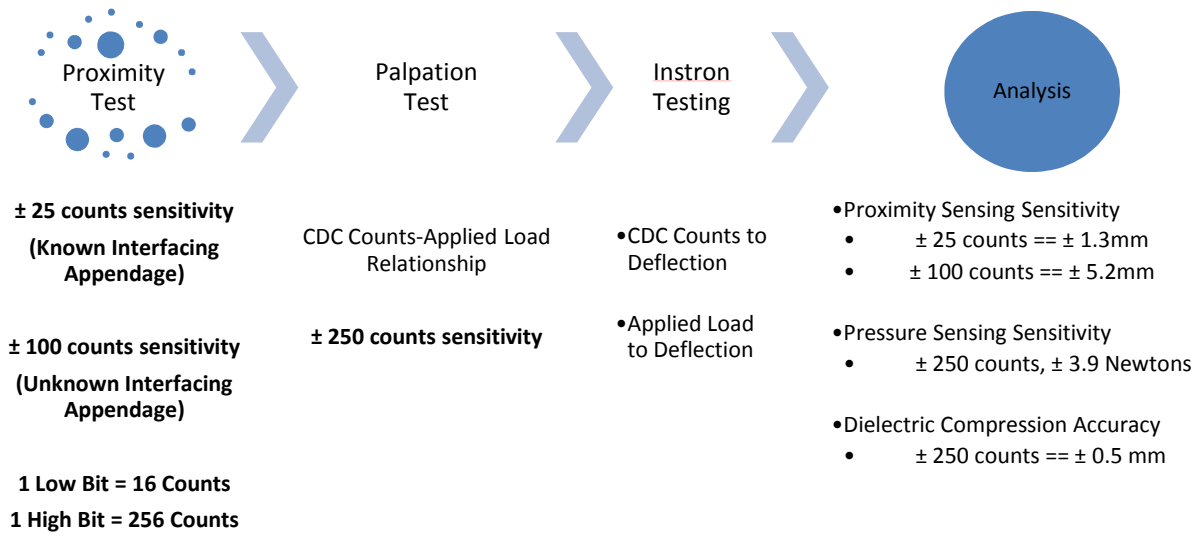

Figure 28. Mutual capacitance proximity and pressure sensing, relative to absolute transition.

Section 4.2 Plantar Proximity and Pressure Sensing Gait Detection Results

The collected data suggests that mutual capacitance can be used for relative plantar proximity and pressure sensing using the sensor layout shown in Figure 29. Figure 30 displays the plantar mutual capacitance changes within the big toe, metatarsal, and heel. Each sensor demonstrated the relative characteristics of the acting plantar region during a gait activity. Figure 31 is the same data with a 20 count moving average. Figure 32 shows the sensor trace

for 1) Heel Strike, 2) Metatarsal Contact, 3) Big Toe Contact, 4) Big Toe Lift-off, 5) Swing, and 6) Heel Strike from the metatarsal sensor. The Metatarsal Heel Strike (6) was a surprise, likely associated with the heel strike pushing the toe of the shoe toward the toe of the foot after swing phase. The proximity of the metatarsal sensor was jolted close to the plantar region during the impact.

Comparing Figure 30 and Figure 31 with respect to system responsiveness, the lower moving average provides a rapid trigger when *instantaneous* timing is required. However, the higher moving average data results in a triggering system based around a consistent motion. This gait data exhibits the prediction variation only in the user's gait: slower when starting and stopping, and consistent in the middle. The results of this are listed in Figure 32. A four sensor plantar system is quadruple-redundant for a generalized gait. While more sensors will provide more redundancy for generalized gait detection, it can also help with *instantaneous* events. When the heel strike shifts the metatarsal sensor closer, the trigger was established at the moment prior to mid-stance.

The counts range was calculated with the static capacitor data to determine the capacitive change in the circuit. In general, 2-4 pF of change was detected. Totaling the normalized load value using an impact value of 1.7 for each sensor provides a load sensing output that can be interpreted as the classic M-curve for pedobarography from Figure 5. The resulting chart is shown in Figure 33. The proximity data has been threshold filtered based on the rapid spike caused by the proximity-pressure sensing transition.

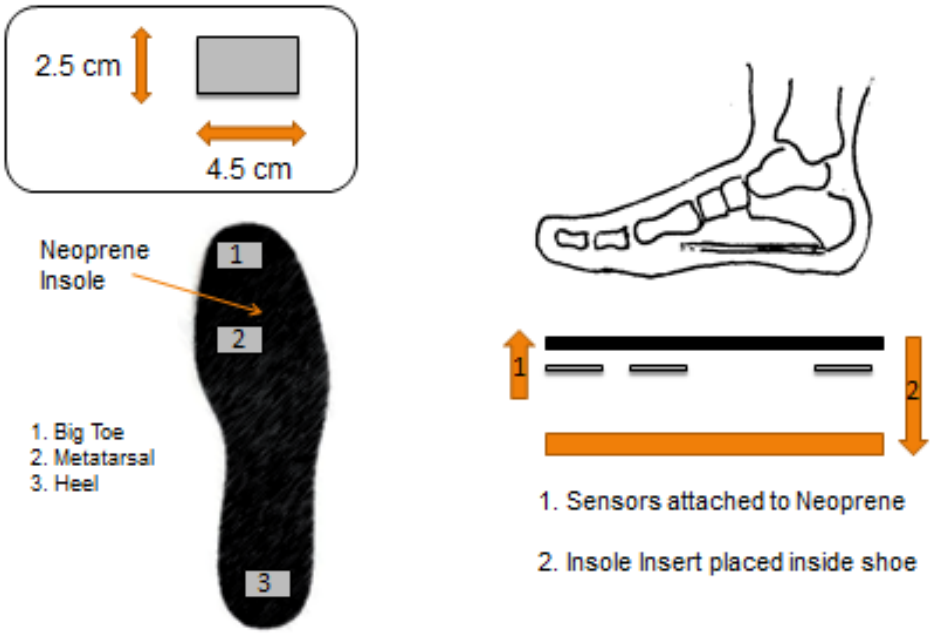

Figure 29. Layout of plantar sensors.

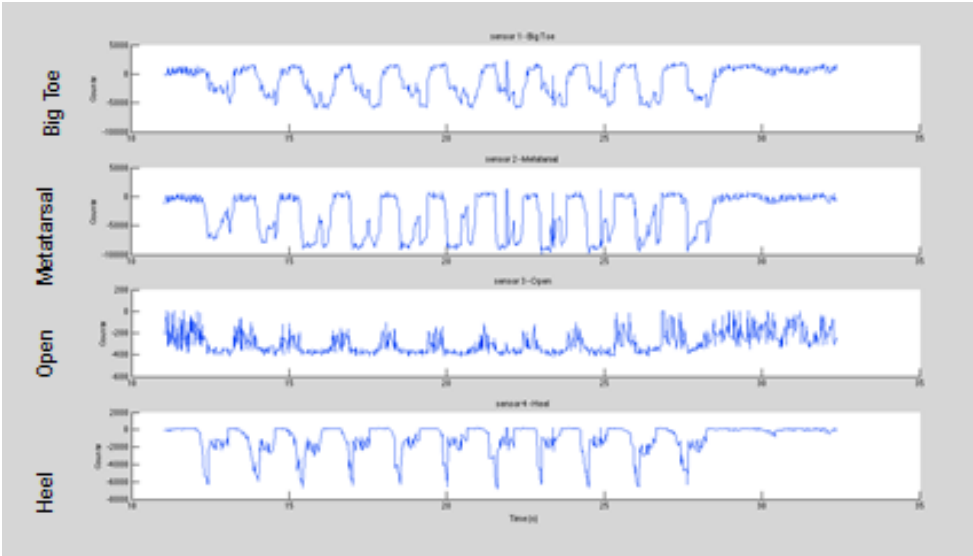

Figure 30. Plantar region mutual capacitive gait unfiltered data. Standing, walking 10 steps, and then standing.

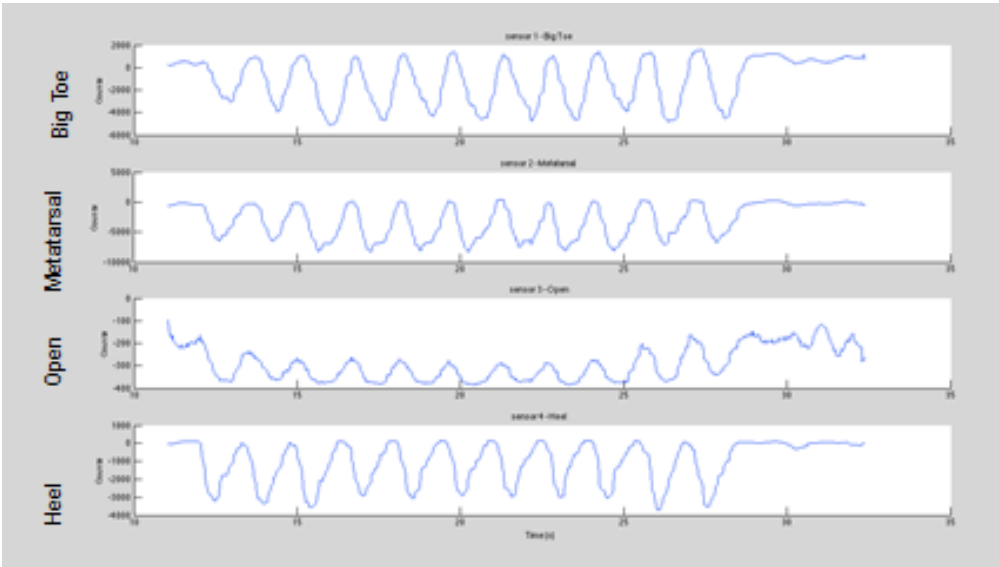

Figure 31. Data filtered with a 20 point moving average. This value is acceptable for general gait detection, but may vary by the particular aspect of the gait being studied.

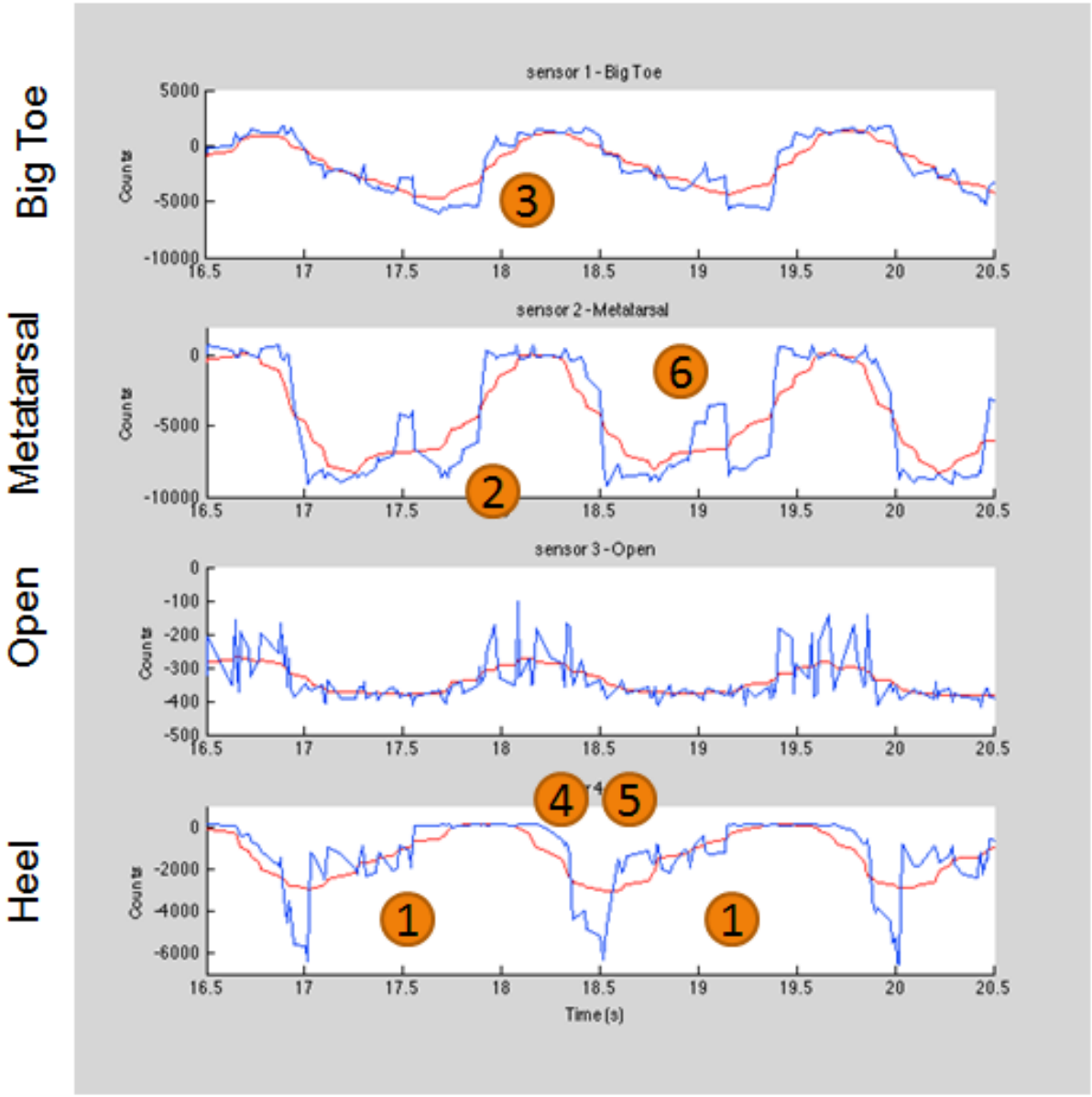

Figure 32. Gait events can be detected with a plantar mutual capacitance sensor: 1) Heel Strike, 2) Metatarsal Contact, 3) Big Toe Contact, 4) Big Toe Lift-off, 5) Swing, and 6) Heel Strike as detected via the Metatarsal sensor.

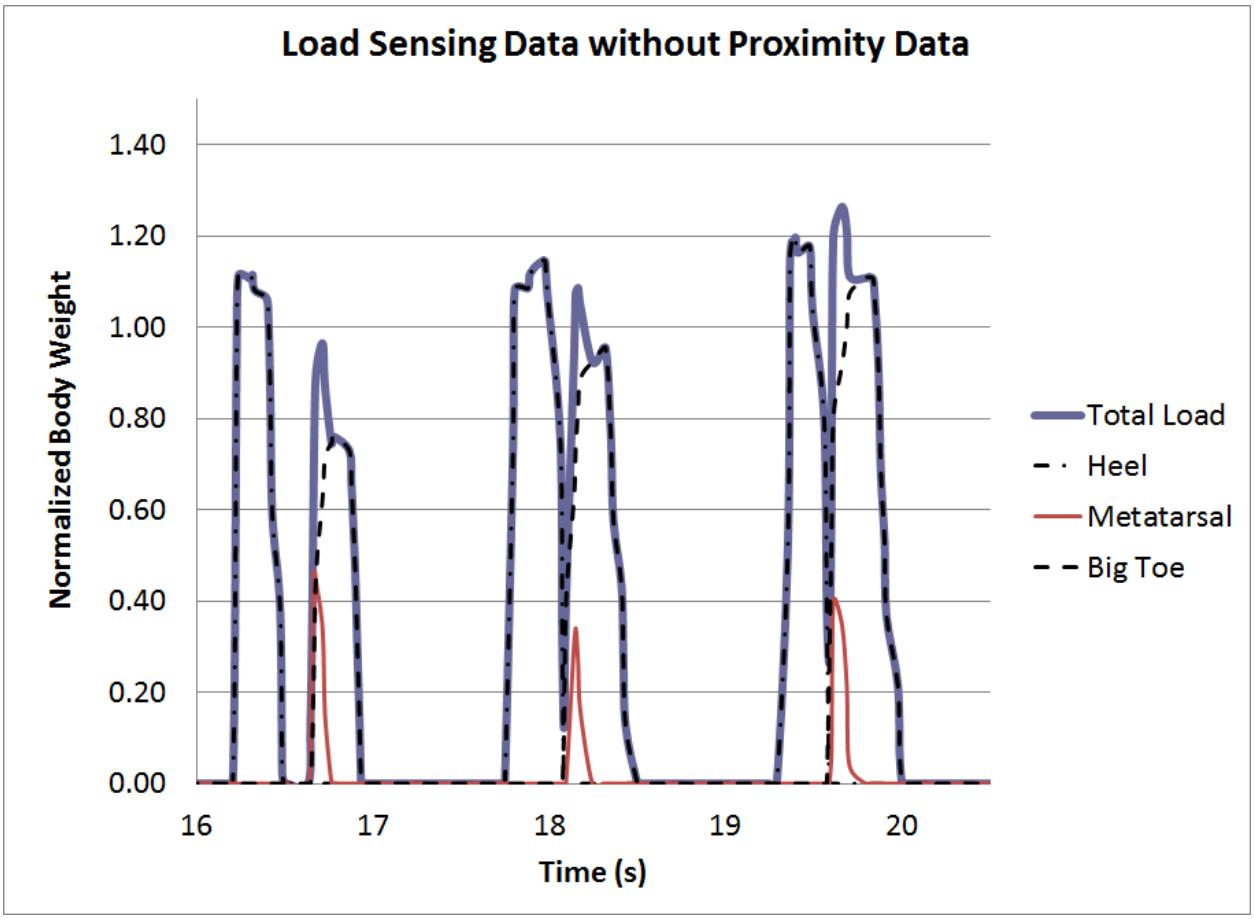

Figure 33. Normalized, totaled plantar load data resulting in classic M-curve.

Chapter 5 Discussion

Plantar region mutual capacitive proximity and pressure sensing can be used for gait detection. This method utilizes sensors under plantar regions to detect when the foot is in contact with a particular sensor. The magnitude of mutual capacitance then depends on the Elastic modulus of the dielectric to calculate an applied load.

This sensor array was designed for detecting a normal walking gait. This technology is robust enough that it can support various gait types. If diabetic, arthritic, or deformed feet are to be studied then the location of the plantar sensors can be either general or specific. Larger sensors that encompass entire plantar regions can provide bulk properties. Higher count, smaller arrays can provide detail information, i.e. horizontal wires across the metatarsal. These sensors can capture the roll of the ball of the foot as it transitions from midstance to toe lift off. These methods can be applied to the heel or toe regions, too.

An additional benefit to mutual capacitive sensing is how easily configurable it is. There are many successful combinations of an elastic dielectric and a flexible conductive plate. The sensors can start as simple homebrew aluminum foil shapes and be transformed to flexible polyester microfabricated sheets. Each is application specific and scalable to the size of the project.

The hardware setup needs iterations of miniaturization. This project used readily available demoboards which sacrifice size for easy integration. An ultimate design would have a small, battery powered microcontroller with multiple CDC ports with integrated Bluetooth. Microcontroller firmware would have to automatically sense the capacitance and adjust the gain in which the dynamic range provides an adequate response. If one has gone to the trouble

of making this portable PCB, then the applications would reach far beyond just Pedobarographic studies. Customized pressure sensing interfaces and proximity gesturing is suddenly available as a generic toolkit and release to the creativity of the masses.

The mutual capacitance between humans and electrical wiring can be used for proximity and pressure sensing applications. Extensive calibration is required to transition the collected data from relative to absolute. This calibration includes bulk modulus mechanical properties of the finger or appendage which is applying the pressure, electric potential of the finger or appendage for the individual, stress-strain curve for the dielectric in compression (or tension), and capacitance-to-CDC counts for the microcontroller. Once these values are understood, either by data collection or statistical confidence, then the sensor becomes an absolute pressure sensor. This relationship is shown in Figure 8. Given the complexity in achieving an absolute proximity and pressure sensor, one may choose to simplify the calibration and apply a relative sensor.

The demonstrated precision in for relative proximity sensing mimics the proven function of the Theremin. The Theremin utilized this technology to use an unfiltered proximity sensing signal to generate an analog sound. If this detection method were variable, the resulting audible sound would also be wavy und variable. If one were to watch an expert playing the Theremin, it would be obvious that the purity of the sound is a function of the stillness of the player's hand as it approaches the antenna. There are numerous future applications that can utilize this technology, including proximity and pressure sensing touchscreens, medical phantom sensing, haptic controls, and medical equipment sensing.

The tests performed within this paper demonstrated satisfactory detection of proximity-to-pressure sensing transition. Additionally, like all other types of sensors, this mutual capacitance sensor must be designed for a specific application, which requires consideration of

sensor size, microcontroller gain and port settings, dielectric selection, and sensor array method.

The calculation of change in capacitiance is independent of area while area is constant. However, area does matter when setting the gain. The dynamic range of the sensor is dependent on the proper amplification without reaching the top of the range. Given the fundamental physics of a finger acting on a sensor with electric potiential, the area would slowly increase from a negligible value. And possibly reaching infinity as the finger nearly presses onto the sensor.

Plantar region mutual capacitive proximity and pressure sensing can be used for gait detection, and the particular method utilized here placed sensors under plantar regions to detect when the foot was in contact with a particular sensor. The magnitude of mutual capacitance then depends on the Elastic modulus of the dielectric to calculate an applied load.

This sensor array was designed for detecting a normal walking gait, although this technology is robust enough to potentially support various types of gait. Specific applications using this plantar region mutual capacitive proximity and pressure sensor involve studying diabetic, arthritic, or deformed feet, and the locations of the plantar sensors could be either general or specific. Larger sensors that encompass entire plantar regions can provide bulk properties, higher count; smaller arrays can provide detailed information (e.g., horizontal wires across the metatarsal). These sensors can capture the roll of the ball of the foot as it transitions from mid-stance phase of the gait cycle to the toe lift-off phase. These methods may be likewise applied to the heel or toe regions to give data respective of those locations of the foot.

This type of sensing is furthermore beneficial in that it is configurable into multiple forms. There are many successful combinations of an elastic dielectric and a flexible conductive plate. The sensors may begin as simple aluminum foil shapes and be transformed into flexible polyester micro-fabricated sheets to microns. Each is application-specific and scalable to the size of the project.

Chapter 6 Future Work

Utilizing mutual capacitance for a proximity and pressure sensor requires refinement to fit the application. The size of the sensor, calibration methods, full or partial dielectric layers, and the type of interaction all play major roles in determining what is being sensed by the electronics. In fact, the software and the firmware on the hardware will even be a factor. From a technical perspective the repeatability and reliability of the sensor and the test setup must be improved. During control load cell and 3rd party sensor setups, the variation in data runs could be explained on either the baseline or the test sensor. Neither was definitive as to the cause. Hence, further research in quantifying this sensing method is first and foremost for developing this technology to transition from relative to absolute.

Looking beyond this early development phase, there are many uses for this sensing method. Within medical phantoms, this sensor can exist as a single wire, array of wires, sensing region, or array of sensing regions. These regions can inform the user or instructor if the proper pressure has been applied or if all regions of interest have been examined. Additionally, each of these sensor types can be integrated with medical device phantoms for to test users for proper sterility methods. If the device is touched while opened, then the sensor would report contact. Also, the proximity sensor would also be able to capture a near-miss, too. Beyond the testing, this method could be integrated into actual devices, as well.

For hardware, a simple wire can be placed under an ultrasound transducer's rubber layer. Now, the sensor can report if contact has been made and if that contact is being applied with the proper pressure, shown in Figure 34. This method is extremely useful if the ultrasound data is used for computer vision and can trigger or withdraw a trigger if the proper pressure is or isn't registered.

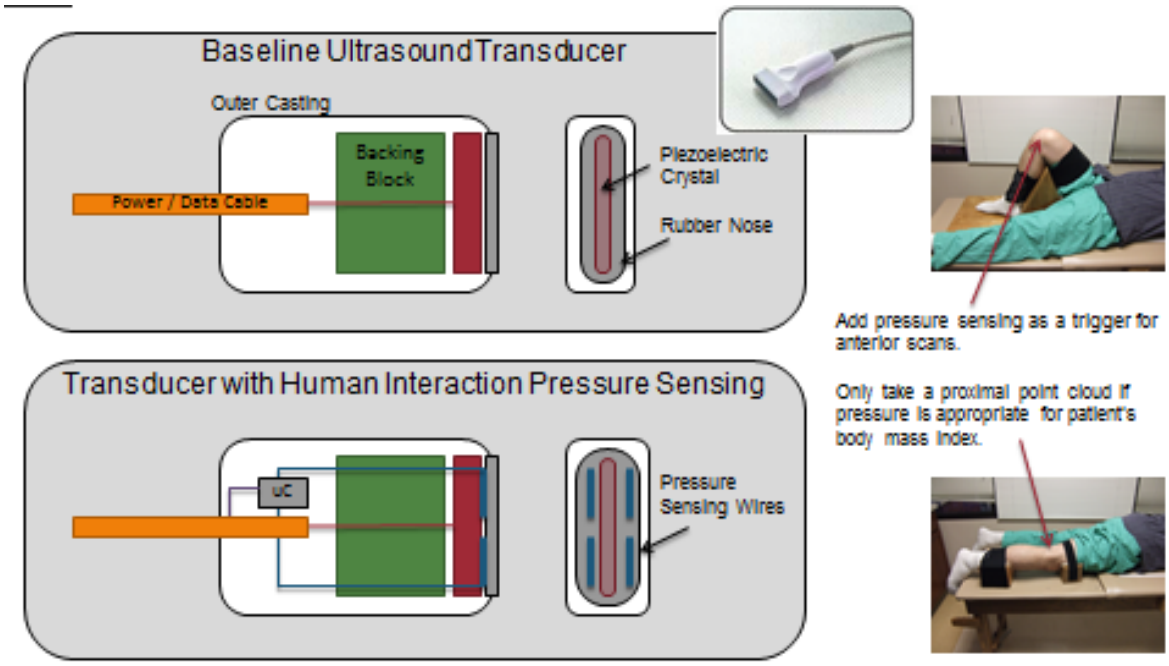

Figure 34. Schematic of typical ultrasound transducer (top) and Schematic of transducer with a mutual capacitive pressure sensor (bottom).

List of References

[1] W. Buller and B. Wilson, "Measurement and Modeling Mutual Capacitance of Electrical Wiring and Humans," *IEEE Transactions on Instrumentation and Measurement,* vol. 55, pp. 1519-1522, 2006.

[2] S. K. T. Togura T., Nakamura, Y., Akashi K., "Long-Range Human-Body-Sensing Modules with Capacitive Sensor," *Fujikura Technical Review,* vol. 2009.

[3] B. D. Cheng J., Lukowicz P., "On Body Capacitive Sensing for a Simple Touchless user Interface," *5th International Workshop on Wearable and Implantable Body Sensor Networks,* vol. The Chinese University of Hong Kong, 2008.

[4] P. W., "Capacitance Sensing in Human Body Contact Applications," *Sensors,* vol. July 1, 2010, 2010.

[5] N. Jonassen, "Human body capacitance: static or dynamic concept? [ESD]," in *Electrical Overstress/Electrostatic Discharge Symposium Proceedings, 1998*, 1998, pp. 111-117.

[6] G. B. a. R. Omote, "Projected-Capacitive Touch Technology," *Information Display,* pp. 16-21, 2010.

[7] M. S. Guide, "Chapter 5 - Capacitance and Dielectrics," vol. web.mit.edu/8.02t/www/materials/StudyGuide/guide05.pdf, 2012.

[8] J. Hughes, "The Clinical Use of Pedobarography," *Acta Orthopaedica Belgica,* vol. 59, 1993.

[9] S. J. Bamberg, A. Y. Benbasat, D. M. Scarborough, D. E. Krebs, and J. A. Paradiso, "Gait analysis using a shoe-integrated wireless sensor system," *IEEE Trans Inf Technol Biomed,* vol. 12, pp. 413-23, Jul 2008.

[10] H. Tuna, M. Birtane, N. Tastekin, and S. Kokino, "Pedobarography and its relation to radiologic erosion scores in rheumatoid arthritis," *Rheumatol Int,* vol. 26, pp. 42-7, Nov 2005.

[11] B. K. Sinclair MF, Rosenbaum D, Bohm S, "Pedobarographic analysis following Ponseti treatment for congenital clubfoot," *Clin Orthop rela,* vol. 467, pp. 1223-1230, 2009.

[12] G. Chan, J. Sampath, F. Miller, E. C. Riddle, M. K. Nagai, and S. J. Kumar, "The role of the dynamic pedobarograph in assessing treatment of cavovarus feet in children with Charcot-Marie-Tooth disease," *J Pediatr Orthop,* vol. 27, pp. 510-6, Jul-Aug 2007.

[13] M. H. J. Young M.J., Veves A.,and Boulton A.J.M., "A comparison of the Musgrave Footprint and optical pedobarograph systems for measuring dynamic foot pressures in diabetic patients," *The Foot,* vol. 3, pp. 62-64, 1993.

[14] A. M. Charles Y.P, Doderlein L., "The use of dynamic pedobarography (DPB) in the post-operative evaluation of pes cavovarus," *Gait & Posture,* vol. 10, p. 70, 1999.

[15] K. H. Park E., Park C., Rha D., Park C., "Dynamic Foot Pressure Measurements for Assessing Foot Deformity in Persons With Spastic Cerebral Palsy," *Arch Phys Med Rehabil,* vol. 87, pp. 703-709, 2006.

[16] M. Lord, D. P. Reynolds, and J. R. Hughes, "Foot pressure measurement: a review of clinical findings," *J Biomed Eng,* vol. 8, pp. 283-94, Oct 1986.

[17] P. N. Han T., Im M., "Quantification of the path of center of pressure (COP) using an F-scan in-shoe transducer," *Gait & Posture,* vol. 10, pp. 248-254, 1999.
[18] Y. S. Hsieh C. J., Hsieh l. F., "Role of Muscle Strength in Dynamic Balance for Subjects with Knee Osteoarthritis," presented at the 4th Kuala Lumpur International Conference on Biomedical Engineering 208, Kuala Lumpur, Malaysia, 2008.
[19] M. J. Hessert, M. Vyas, J. Leach, K. Hu, L. A. Lipsitz, and V. Novak, "Foot pressure distribution during walking in young and old adults," *BMC Geriatr,* vol. 5, p. 8, 2005.
[20] E. Kul-Panza and N. Berker, "Pedobarographic findings in patients with knee osteoarthritis," *Am J Phys Med Rehabil,* vol. 85, pp. 228-33, Mar 2006.
[21] T. M. Patil S., Chaskar U., "Development of Planter Foot Pressure Distribution System Using Flexi Force Sensors," *Sensors & Transducers Journal,* vol. 108, pp. 73-79, 2009.
[22] I. P. Pappas, M. R. Popovic, T. Keller, V. Dietz, and M. Morari, "A reliable gait phase detection system," *IEEE Trans Neural Syst Rehabil Eng,* vol. 9, pp. 113-25, Jun 2001.
[23] G. Fullen, "System for Continuously Measuring Forces Applied to the Foot," USA Patent, 1994.
[24] R. Podoloff, "Flexible Tactile Sensor for Measuring Foot Pressure Distributions and for Gaskets," 1991.
[25] Available: http://www.silabs.com/products/mcu/capacitivesense/Pages/C8051F99x.aspx

Vita

Jonathan William Huber was born in Pittsburg, PA, to the parents of J. William and Nancy Huber. He is the middle child between two sisters Janine and Kari. He attended North Laurel High School in London, KY. Jon reentered the Biomedical Engineering Department at the University of Tennessee, Knoxville after a ten year career as an engineer within various technology industries. Upon acceptance into the doctoral program, he was the first non-Electrical Engineer to be awarded the Ronald Nutt Fellowship for Distinguished Fellows for 2009 and 2010. He was introduced to Dr. Mohamed Mahfouz in 2009 and began to study many topics including capacitive pressure sensing. He graduated with a Bachelors of Science degree in May 1998 in Engineering Science with a Concentration in Biomedical Engineering and a Masters of Science in Summer 2003 in Engineering Science. All degrees have been completed at the University of Tennessee, Knoxville. His next step is to continue to research and to innovate while he is leading a R&D team charted to develop a next generation proton therapy system for ProNova Solutions, LLC in Knoxville, TN.